Branching ratios, forward-backward asymmetries, and angular distributions of $B \to K_2^* l^+ l^-$ in the standard model and two new physics scenarios

Run-Hui Li,[1,2] Cai-Dian Lü,[1] and Wei Wang[3,*]

[1]*Institute of High Energy Physics, P.O. Box 918(4), Beijing 100049, People's Republic of China*
[2]*Department of Physics & IPAP, Yonsei University, Seoul 120-479, Korea*
[3]*Deutsches Elektronen-Synchrotron DESY, Hamburg 22607, Germany*

(Received 16 December 2010; published 25 February 2011)

We analyze the $B \to K_2^*(\to K\pi) l^+ l^-$ (with $l = e, \mu, \tau$) decay in the standard model and two new physics scenarios: the vectorlike quark model and family nonuniversal Z' models. We derive the differential angular distributions using the recently calculated form factors in the perturbative QCD approach. Branching ratios, polarizations, forward-backward asymmetries, and transversity amplitudes are predicted, from which we find a promising prospective to observe this channel in future experiments. We update the constraints on effective Wilson coefficients and/or free parameters in these two new physics scenarios by making use of the $B \to K^* l^+ l^-$ and $b \to s l^+ l^-$ experimental data. Their impact on $B \to K_2^* l^+ l^-$ is subsequently explored and, in particular, the zero-crossing point for the forward-backward asymmetry in these new physics scenarios can sizably deviate from the standard model. In addition we also generalize the analysis to a similar mode, $B_s \to f_2'(1525)(\to K^+ K^-) l^+ l^-$.

DOI: 10.1103/PhysRevD.83.034034 PACS numbers: 13.20.He, 12.39.St, 14.40.Be

I. INTRODUCTION

Discoveries of new degrees of freedom at the TeV energy scale, with contributions to our understanding of the origin of the electroweak symmetry breaking, can proceed in two different ways. One is a direct search of the Higgs boson, the last piece needed to complete the standard model (SM), and particles beyond the SM, to establish new physics (NP) theories. The other effort, which is ongoing, is to investigate processes in which the SM is tested with higher experimental and theoretical precision. In the latter category, rare B decays are among the ideal probes. Besides constraints on the Cabibbo-Kobayashi-Maskawa (CKM) matrix, including apexes and angles of the unitary triangle, which have been contributed by semileptonic $b \to u/c$ and nonleptonic B decays, respectively, the electroweak interaction structure can also be probed by, for instance, the $b \to s\gamma$ and $b \to s l^+ l^-$ modes which are induced by loop effects in the SM and therefore sensitive to the NP interactions.

Unlike $b \to s\gamma$ and $B \to K^*\gamma$ which have only limited physical observables, $b \to s l^+ l^-$, and especially $B \to K^* l^+ l^-$, with a number of observables accessible, provides a wealth of information of weak interactions, ranging from the forward-backward asymmetries (FBAs), isospin symmetries, and polarizations to a full angular analysis. The last barrier to accessing this mode, the low statistics with a branching fraction of the order 10^{-6}, is being cleared by B factories and the hadron collider at Tevatron [1–3]. The ongoing LHCb experiment can accumulate 6200 events per nominal running year of 2 fb^{-1} with $\sqrt{s} = 14$ TeV [4], which allows one to probe the short-distance physics at an unprecedented level. For instance, the sensitivity to the zero-crossing point of FBAs can be reduced to 0.5 GeV^2 and might be further improved as 0.1 GeV^2 after the upgrade [5]. This provides a good sensitivity to discriminate between the SM and different models of new physics. There are also a lot of opportunities at the Super B factory [6]. Because of these virtues, theoretical research interests in this mode have exploded and the precision is highly improved; see Refs. [7–22] for an incomplete list.

Toward the direction to elucidate the electroweak interaction, $B \to K^* l^+ l^-$ and its $SU(3)$-related mode $B_s \to \phi l^+ l^-$ are not unique. In this work, we shall point out that $B \to K_2^*(1430) l^+ l^-$ and the B_s counterpart $B_s \to f_2'(1525) l^+ l^-$,[1] which so far have not been investigated in detail [23–26], are also useful in several aspects. Because of the similarities between K^* and K_2^*, all experimental techniques for $B \to K^* l^+ l^-$ are adjustable to $B \to K_2^* l^+ l^-$. The main decay product of K_2^* is a pair consisting of a charged kaon and a pion which are easily detected on the LHCb. Moreover, as we will show in the following, based on either a direct computation in the perturbative QCD approach [27] or the implication of experimental data on the $B \to K_2^*\gamma$ process, the branching ratio (BR) of $B \to K_2^* l^+ l^-$ is found to be sizable. Therefore, thousands of signal events can be accumulated on the LHCb per nominal running year.

As a consequence of the unitarity of the quark mixing matrix, the tree-level flavor-changing neutral current (FCNC) is forbidden in the SM. When higher order corrections are taken into account, $b \to s l^+ l^-$ arises from the photonic penguin, the Z penguin, and the W-box diagram. The large mass scale of virtual states leads to tiny Wilson

*wei.wang@desy.de

[1]Hereafter, we will use K_2^* and f_2' to abbreviate $K_2^*(1430)$ and $f_2'(1525)$.

coefficients in b quark decays and thus $b \to s l^+ l^-$ would be sensitive to the potential NP effects. In certain NP scenarios, new effective operators out of the SM scope can emerge, but in other scenarios, only Wilson coefficients for effective operators are modified. In the latter category, the vectorlike quark model (VQM) [28–36] and family nonuniversal Z' models [37–42] are simplest and therefore of theoretical interest. In this work we shall also elaborate on the impact of these models on $B \to K_2^* l^+ l^-$.

The rest of the paper is organized as follows. In Sec. II, we collect the necessary hadronic inputs, namely, form factors. Section II contains the analytic formulas for differential decay distributions and integrated quantities. In Sec. IV, we give a brief overview of two NP models whose effects we will study. Section V contains our phenomenological analysis: the predictions in the SM, an update of the constraints on the VQM and Z' model parameters, and the NP effect on the physical quantities. We conclude in the last section. In the appendices, we give the effective Hamiltonian in the SM and the helicity amplitude method.

II. $B \to K_2$ FORM FACTORS

$B \to K_2^* l^+ l^-$ decay amplitudes contain two separate parts. Short-distance physics, in which contributions at the weak scale μ_W are calculated by perturbation theory and the evolution between m_W and the b quark mass scale m_b is organized by the renormalization group. These degrees of freedom are incorporated into Wilson coefficients and the obtained effective Hamiltonian responsible for $b \to s l^+ l^-$ in Appendix A. The low-energy effect characterizes the long-distance physics and will be parametrized by hadronic matrix elements of effective operators, which are usually reduced to heavy-to-light form factors in semileptonic B decays.

The spin-2 polarization tensor, which satisfies $\epsilon_{\mu\nu} P_2^\nu = 0$, with P_2 being the momentum, is symmetric and traceless. It can be constructed via the spin-1 polarization vector ϵ:

$$\begin{aligned}
\epsilon_{\mu\nu}(\pm 2) &= \epsilon_\mu(\pm)\epsilon_\nu(\pm), \\
\epsilon_{\mu\nu}(\pm 1) &= \frac{1}{\sqrt{2}}[\epsilon_\mu(\pm)\epsilon_\nu(0) + \epsilon_\nu(\pm)\epsilon_\mu(0)], \\
\epsilon_{\mu\nu}(0) &= \frac{1}{\sqrt{6}}[\epsilon_\mu(+)\epsilon_\nu(-) + \epsilon_\nu(+)\epsilon_\mu(-)] \\
&\quad + \sqrt{\frac{2}{3}}\epsilon_\mu(0)\epsilon_\nu(0).
\end{aligned} \tag{1}$$

In the case of the tensor meson moving on the z axis, the explicit structures of ϵ in the ordinary coordinate frame are chosen as

$$\begin{aligned}
\epsilon_\mu(0) &= \frac{1}{m_{K_2^*}}(|\vec{p}_{K_2^*}|, 0, 0, E_{K_2^*}), \\
\epsilon_\mu(\pm) &= \frac{1}{\sqrt{2}}(0, \mp 1, -i, 0),
\end{aligned} \tag{2}$$

where $E_{K_2^*}$ and $\vec{p}_{K_2^*}$ are the energy and the momentum magnitude of K_2^* in the B meson rest frame, respectively. In the following calculation, it is convenient to introduce a new polarization vector ϵ_T,

$$\epsilon_{T\mu}(h) = \frac{1}{m_B}\epsilon_{\mu\nu}(h) P_B^\nu, \tag{3}$$

which satisfies

$$\epsilon_{T\mu}(\pm 2) = 0, \qquad \epsilon_{T\mu}(\pm 1) = \frac{1}{m_B}\frac{1}{\sqrt{2}}\epsilon(0)\cdot P_B \epsilon_\mu(\pm), \qquad \epsilon_{T\mu}(0) = \frac{1}{m_B}\sqrt{\frac{2}{3}}\epsilon(0)\cdot P_B \epsilon_\mu(0). \tag{4}$$

The contraction is evaluated as $\epsilon(0)\cdot P_B/m_B = |\vec{p}_{K_2^*}|/m_{K_2^*}$, and thus we can see that the new vector ϵ_T plays a similar role to the ordinary polarization vector ϵ, regardless of the dimensionless constants $\frac{1}{\sqrt{2}}|\vec{p}_{K_2^*}|/m_{K_2^*}$ or $\sqrt{\frac{2}{3}}|\vec{p}_{K_2^*}|/m_{K_2^*}$.

The parametrization of $B \to K_2^*$ form factors is analogous to the $B \to K^*$ ones [25–27,43],

$$\begin{aligned}
\langle K_2^*(P_2,\epsilon)|\bar{s}\gamma^\mu b|\bar{B}(P_B)\rangle &= -\frac{2V(q^2)}{m_B + m_{K_2^*}}\epsilon^{\mu\nu\rho\sigma}\epsilon^*_{T\nu}P_{B\rho}P_{2\sigma}, \\
\langle K_2^*(P_2,\epsilon)|\bar{s}\gamma^\mu\gamma_5 b|\bar{B}(P_B)\rangle &= 2im_{K_2^*}A_0(q^2)\frac{\epsilon_T^*\cdot q}{q^2}q^\mu + i(m_B + m_{K_2^*})A_1(q^2)\left[\epsilon^*_{T\mu} - \frac{\epsilon_T^*\cdot q}{q^2}q^\mu\right] \\
&\quad - iA_2(q^2)\frac{\epsilon_T^*\cdot q}{m_B + m_{K_2^*}}\left[P^\mu - \frac{m_B^2 - m_{K_2^*}^2}{q^2}q^\mu\right], \\
\langle K_2^*(P_2,\epsilon)|\bar{s}\sigma^{\mu\nu}q_\nu b|\bar{B}(P_B)\rangle &= -2iT_1(q^2)\epsilon^{\mu\nu\rho\sigma}\epsilon^*_{T\nu}P_{B\rho}P_{2\sigma}, \\
\langle K_2^*(P_2,\epsilon)|\bar{s}\sigma^{\mu\nu}\gamma_5 q_\nu b|\bar{B}(P_B)\rangle &= T_2(q^2)[(m_B^2 - m_{K_2^*}^2)\epsilon^*_{T\mu} - \epsilon_T^*\cdot q P^\mu] + T_3(q^2)\epsilon_T^*\cdot q\left[q^\mu - \frac{q^2}{m_B^2 - m_{K_2^*}^2}P^\mu\right],
\end{aligned} \tag{5}$$

where $q = P_B - P_2$, $P = P_B + P_2$. We also have the relation $2m_{K_2^*}A_0(0) = (m_B + m_{K_2^*})A_1(0) - (m_B - m_{K_2^*})A_2(0)$ in order to smear the pole at $q^2 = 0$.

Using the newly studied light-cone distribution amplitudes [44], we have computed $B \to K_2^*$ form factors [27] in the perturbative QCD approach (PQCD) [45]. At the leading power, our predictions are found to obey the nontrivial relations derived from the large energy symmetry. This consistency may imply that the PQCD results for the form factors are reliable and therefore suitable for the study of the semileptonic B decays. The recent computation in light-cone QCD sum rules [43] is also consistent with ours. Results in the light-cone sum rules (LCSR) in conjunction with B-meson wave functions [46], however, are too large and thus not favored by the $B \to K_2^*\gamma$ data. In our work the $B \to K_2^*$ form factors are q^2 distributed as [27]

$$F(q^2) = \frac{F(0)}{(1 - q^2/m_B^2)(1 - a(q^2/m_B^2) + b(q^2/m_B^2)^2)}, \quad (6)$$

where F denotes a generic form factor among A_0, A_1, V, T_{1-3}. Neglecting higher power corrections, A_2 is related to A_0 and A_1 by

$$A_2(q^2) = \frac{m_B + m_{K_2^*}}{m_B^2 - q^2}[(m_B + m_{K_2^*})A_1(q^2) - 2m_{K_2^*}A_0(q^2)]. \quad (7)$$

Numerical results for the $B \to K_2^*$ and $B_s \to f_2'(1525)$ form factors at the maximal recoil point and the two fitted parameters a, b are collected in Table I. The two kinds of errors are from (1) decay constants of the B meson and shape parameter ω_b and (2) $\Lambda_{\rm QCD}$, the scales ts, and the threshold resummation parameter c [27].

TABLE I. $B \to K_2^*$ and $B_s \to f_2'(1525)$ form factors in the PQCD approach. $F(0)$ denotes results at the point $q^2 = 0$, while a, b are the parameters in the parametrization shown in Eq. (6). The two kinds of errors are from (1) decay constants of the B meson and the shape parameter ω_b and (2) $\Lambda_{\rm QCD}$, factorization scales ts, and the threshold resummation parameter c.

F	$F(0)$	a	b
$V^{BK_2^*}$	$0.21^{+0.04+0.05}_{-0.04-0.03}$	$1.73^{+0.02+0.05}_{-0.02-0.03}$	$0.66^{+0.04+0.07}_{-0.05-0.01}$
$A_0^{BK_2^*}$	$0.18^{+0.04+0.04}_{-0.03-0.03}$	$1.70^{+0.00+0.05}_{-0.02-0.07}$	$0.64^{+0.00+0.04}_{-0.06-0.10}$
$A_1^{BK_2^*}$	$0.13^{+0.03+0.03}_{-0.02-0.02}$	$0.78^{+0.01+0.05}_{-0.01-0.04}$	$-0.11^{+0.02+0.04}_{-0.03-0.02}$
$A_2^{BK_2^*}$	$0.08^{+0.02+0.02}_{-0.02-0.01}$	...	...
$T_1^{BK_2^*}$	$0.17^{+0.04+0.04}_{-0.03-0.03}$	$1.73^{+0.00+0.05}_{-0.03-0.07}$	$0.69^{+0.00+0.05}_{-0.08-0.11}$
$T_2^{BK_2^*}$	$0.17^{+0.03+0.04}_{-0.03-0.03}$	$0.79^{+0.00+0.02}_{-0.04-0.09}$	$-0.06^{+0.00+0.00}_{-0.10-0.16}$
$T_3^{BK_2^*}$	$0.14^{+0.03+0.03}_{-0.03-0.02}$	$1.61^{+0.01+0.09}_{-0.00-0.04}$	$0.52^{+0.05+0.15}_{-0.01-0.01}$
$V^{B_sf_2'}$	$0.20^{+0.04+0.05}_{-0.03-0.03}$	$1.75^{+0.02+0.05}_{-0.00-0.03}$	$0.69^{+0.05+0.08}_{-0.01-0.01}$
$A_0^{B_sf_2'}$	$0.16^{+0.03+0.03}_{-0.02-0.02}$	$1.69^{+0.00+0.04}_{-0.01-0.03}$	$0.64^{+0.00+0.01}_{-0.04-0.02}$
$A_1^{B_sf_2'}$	$0.12^{+0.02+0.03}_{-0.02-0.02}$	$0.80^{+0.02+0.07}_{-0.00-0.03}$	$-0.11^{+0.05+0.09}_{-0.00-0.00}$
$A_2^{B_sf_2'}$	$0.09^{+0.02+0.02}_{-0.01-0.01}$	...	...
$T_1^{B_sf_2'}$	$0.16^{+0.03+0.04}_{-0.03-0.02}$	$1.75^{+0.01+0.05}_{-0.00-0.05}$	$0.71^{+0.03+0.06}_{-0.01-0.08}$
$T_2^{B_sf_2'}$	$0.16^{+0.03+0.04}_{-0.03-0.02}$	$0.82^{+0.00+0.04}_{-0.04-0.06}$	$-0.08^{+0.00+0.03}_{-0.09-0.08}$
$T_3^{B_sf_2'}$	$0.13^{+0.03+0.03}_{-0.02-0.02}$	$1.64^{+0.02+0.06}_{-0.00-0.06}$	$0.57^{+0.04+0.05}_{-0.01-0.09}$

III. DIFFERENTIAL DECAY DISTRIBUTIONS AND SPIN AMPLITUDES

In this section, we will discuss the kinematics of the quasi four-body decay $B \to K_2^*(\to K\pi)l^+l^-$, define angular observables, and collect the explicit formulas of helicity amplitudes and/or transversity amplitudes.

A. Differential decay distribution

At the quark level, the decay amplitude for $b \to sl^+l^-$ is expressed as

$$\mathcal{M}(b \to sl^+l^-) = \frac{G_F}{\sqrt{2}}\frac{\alpha_{\rm em}}{\pi}V_{tb}V_{ts}^* \times \Big(\frac{C_9 + C_{10}}{4}[\bar{s}b]_{V-A}[\bar{l}l]_{V+A} + \frac{C_9 - C_{10}}{4}[\bar{s}b]_{V-A}[\bar{l}l]_{V-A} + C_{7L}m_b[\bar{s}i\sigma_{\mu\nu}(1+\gamma_5)b]\frac{q^\mu}{q^2} \times [\bar{l}\gamma^\nu l] + C_{7R}m_b[\bar{s}i\sigma_{\mu\nu}(1-\gamma_5)b]\frac{q^\mu}{q^2} \times [\bar{l}\gamma^\nu l]\Big), \quad (8)$$

where $C_{7L} = C_7$ and $C_{7R} = \frac{m_s}{m_b}C_{7L}$ in the SM. Sandwiching Eq. (8) between the initial and final states and replacing the spinor product $[\bar{s}b]$ by hadronic matrix elements, one obtains the decay amplitude for the hadronic B process. For the process under scrutiny in this work, the decay observed in the experiment is actually $B \to K_2^*(\to K\pi)l^+l^-$, which is a quasi four-body decay. The convention on the kinematics is illustrated in Fig. 1. The moving direction of K_2^* in the B meson rest frame is chosen as the z axis. The polar angle θ_K (θ_l) is defined as the angle between the flight direction of K^- (μ^-) and the z axis in the K_2^* (lepton pair) rest frame. ϕ is the angle defined by decay planes of K_2^* and the lepton pair.

Using the technique of helicity amplitudes described in Appendix B, we obtain the partial decay width

$$\frac{d^4\Gamma}{dq^2 d\cos\theta_K d\cos\theta_l d\phi} = \frac{3}{8}|\mathcal{M}_B|^2, \quad (9)$$

with the mass correction factor $\beta_l = \sqrt{1 - 4m_l^2/q^2}$. The function $|\mathcal{M}_B|^2$ is decomposed into 11 terms,

$$|\mathcal{M}_B|^2 = [I_1^c C^2 + 2I_1^s S^2 + (I_2^c C^2 + 2I_2^s S^2)\cos(2\theta_l) + 2I_3 S^2 \sin^2\theta_l \cos(2\phi) + 2\sqrt{2} I_4 CS \sin(2\theta_l)\cos\phi + 2\sqrt{2} I_5 CS \sin(\theta_l)\cos\phi + 2I_6 S^2 \cos\theta_l + 2\sqrt{2} I_7 CS \sin(\theta_l)\sin\phi + 2\sqrt{2} I_8 CS \sin(2\theta_l)\sin\phi + 2I_9 S^2 \sin^2\theta_l \sin(2\phi)], \tag{10}$$

with the angular coefficients

$$\begin{aligned}
I_1^c &= (|A_{L0}|^2 + |A_{R0}|^2) + 8\frac{m_l^2}{q^2}\,\mathrm{Re}[A_{L0}A_{R0}^*] + 4\frac{m_l^2}{q^2}|A_t|^2,\\
I_1^s &= \frac{3}{4}[|A_{L\perp}|^2 + |A_{L\parallel}|^2 + |A_{R\perp}|^2 + |A_{R\parallel}|^2]\left(1 - \frac{4m_l^2}{3q^2}\right) + \frac{4m_l^2}{q^2}\,\mathrm{Re}[A_{L\perp}A_{R\perp}^* + A_{L\parallel}A_{R\parallel}^*],\\
I_2^c &= -\beta_l^2(|A_{L0}|^2 + |A_{R0}|^2),\\
I_2^s &= \frac{1}{4}\beta_l^2(|A_{L\perp}|^2 + |A_{L\parallel}|^2 + |A_{R\perp}|^2 + |A_{R\parallel}|^2),\\
I_3 &= \frac{1}{2}\beta_l^2(|A_{L\perp}|^2 - |A_{L\parallel}|^2 + |A_{R\perp}|^2 - |A_{R\parallel}|^2),\\
I_4 &= \frac{1}{\sqrt{2}}\beta_l^2[\mathrm{Re}(A_{L0}A_{L\parallel}^*) + \mathrm{Re}(A_{R0}A_{R\parallel}^*)], \qquad I_5 = \sqrt{2}\beta_l[\mathrm{Re}(A_{L0}A_{L\perp}^*) - \mathrm{Re}(A_{R0}A_{R\perp}^*)],\\
I_6 &= 2\beta_l[\mathrm{Re}(A_{L\parallel}A_{L\perp}^*) - \mathrm{Re}(A_{R\parallel}A_{R\perp}^*)], \qquad I_7 = \sqrt{2}\beta_l[\mathrm{Im}(A_{L0}A_{L\parallel}^*) - \mathrm{Im}(A_{R0}A_{R\parallel}^*)],\\
I_8 &= \frac{1}{\sqrt{2}}\beta_l^2[\mathrm{Im}(A_{L0}A_{L\perp}^*) + \mathrm{Im}(A_{R0}A_{R\perp}^*)], \qquad I_9 = \beta_l^2[\mathrm{Im}(A_{L\parallel}A_{L\perp}^*) + \mathrm{Im}(A_{R\parallel}A_{R\perp}^*)].
\end{aligned} \tag{11}$$

$C = C(K_2^*)$ and $S = S(K_2^*)$ for $B \to K_2^* l^+ l^-$. Without higher order QCD corrections, I_7 is zero and I_8, I_9 are tiny in the SM; this is because only C_9 has an imaginary part. In this sense, these coefficients can be chosen as an ideal window to probe new physics signals.

The amplitudes A_i are generated from the hadronic $B \to K_2^* V$ amplitudes $\mathcal{H}_i$ through $A_i = \sqrt{\frac{\sqrt{\lambda} q^2 \beta_l}{3\cdot 32 m_B^3 \pi^3}\mathcal{B}(K_2^* \to K\pi)}\,\mathcal{H}_i$,

$$\begin{aligned}
A_{L0} &= N_{K_2^*}\frac{\sqrt{\lambda}}{\sqrt{6} m_B m_{K_2^*}}\frac{1}{2m_{K_2^*}\sqrt{q^2}}\Bigg[(C_9 - C_{10})\Bigg[(m_B^2 - m_{K_2^*}^2 - q^2)(m_B + m_{K_2^*})A_1 - \frac{\lambda}{m_B + m_{K_2^*}}A_2\Bigg]\\
&\quad + 2m_b(C_{7L} - C_{7R})\Bigg[(m_B^2 + 3m_{K_2^*}^2 - q^2)T_2 - \frac{\lambda}{m_B^2 - m_{K_2^*}^2}T_3\Bigg]\Bigg],\\
A_{L\pm} &= N_{K_2^*}\frac{\sqrt{\lambda}}{\sqrt{8} m_B m_{K_2^*}}\Bigg[(C_9 - C_{10})[(m_B + m_{K_2^*})A_1 \mp \frac{\sqrt{\lambda}}{m_B + m_{K_2^*}}V\Bigg] - \frac{2m_b(C_{7L} + C_{7R})}{q^2}(\pm\sqrt{\lambda}T_1)\\
&\quad + \frac{2m_b(C_{7L} - C_{7R})}{q^2}(m_B^2 - m_{K_2^*}^2)T_2\Bigg],\\
A_{Lt} &= N_{K_2^*}\frac{\sqrt{\lambda}}{\sqrt{6} m_B m_{K_2^*}}(C_9 - C_{10})\frac{\sqrt{\lambda}}{\sqrt{q^2}}A_0,
\end{aligned} \tag{12}$$

with $N_{K_2^*} = [\frac{G_F^2\alpha_{\mathrm{em}}^2}{3\cdot 2^{10}\pi^5 m_B^3}|V_{tb}V_{ts}^*|^2 q^2 \lambda^{1/2}(1 - \frac{4m_l^2}{q^2})^{1/2}\mathcal{B}(K_2^* \to K\pi)]^{1/2}$. For convenience, we have introduced transversity amplitudes as

$$\begin{aligned}
A_{L\perp/\parallel} &= \frac{1}{\sqrt{2}}(A_{L+} \mp A_{L-}),\\
A_{L\perp} &= -\sqrt{2}\frac{\sqrt{\lambda}}{\sqrt{8} m_B m_{K_2^*}}N_{K_2^*}\Bigg[(C_9 - C_{10})\frac{\sqrt{\lambda}V}{m_B + m_{K_2^*}} + \frac{2m_b(C_{7L} + C_{7R})}{q^2}\sqrt{\lambda}T_1\Bigg],\\
A_{L\parallel} &= \sqrt{2}\frac{\sqrt{\lambda}}{\sqrt{8} m_B m_{K_2^*}}N_{K_2^*}\Bigg[(C_9 - C_{10})(m_B + m_{K_2^*})A_1 + \frac{2m_b(C_{7L} - C_{7R})}{q^2}(m_B^2 - m_{K_2^*}^2)T_2\Bigg],
\end{aligned} \tag{13}$$

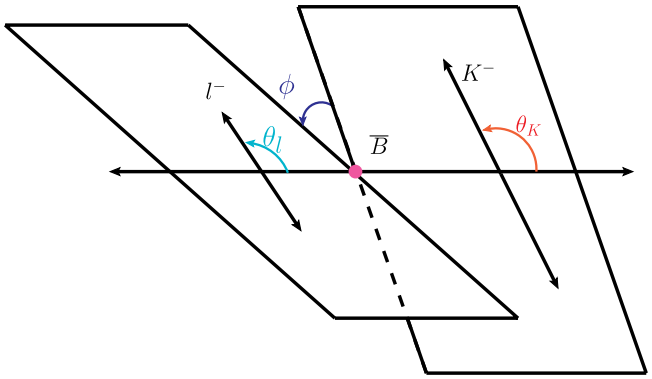

FIG. 1 (color online). Kinematics variables in the $\bar{B} \to \bar{K}_2^*(\to K^-\pi^+)l^+l^-$ process. The moving direction of K_2^* in the B rest frame is chosen as the z axis. The polar angle θ_K (θ_l) is defined as the angle between the flight direction of K^- (μ^-) and the z axis in the K_2^* (lepton pair) rest frame. The convention also applies to the $B_s \to f_2'(\to K^+K^-)l^+l^-$ transition.

and the right-handed decay amplitudes are similar,

$$A_{Ri} = A_{Li}|_{C_{10}\to -C_{10}}. \tag{14}$$

The combination of the timelike decay amplitudes is used in the differential distribution

$$A_t = A_{Rt} - A_{Lt} = 2N_{K_2^*}\frac{\sqrt{\lambda}}{\sqrt{6}m_B m_{K_2^*}} C_{10}\frac{\sqrt{\lambda}}{\sqrt{q^2}}A_0. \tag{15}$$

B. Dilepton spectrum distribution

Integrating out the angles θ_l, θ_K, and ϕ, we obtain the dilepton mass spectrum

$$\frac{d\Gamma}{dq^2} = \frac{1}{4}(3I_1^c + 6I_1^s - I_2^c - 2I_2^s), \tag{16}$$

and its expression in the massless limit,

$$\frac{d\Gamma_i}{dq^2} = (|A_{Li}|^2 + |A_{Ri}|^2), \tag{17}$$

with $i = 0, \pm 1$ or $i = 0, \perp, \parallel$. After some manipulations in Appendix B, the correspondence of the above equations and Eq. (20) with results in Ref. [25] can be shown.

C. Polarization distribution

The longitudinal polarization distribution for $\bar{B} \to \bar{K}_2^* l^+ l^-$ is defined as

$$\frac{df_L}{dq^2} \equiv \frac{d\Gamma_0}{dq^2}\Big/\frac{d\Gamma}{dq^2} = \frac{3I_1^c - I_2^c}{3I_1^c + 6I_1^s - I_2^c - 2I_2^s}, \tag{18}$$

in which $\frac{d\Gamma_0}{dq^2}$ can be reduced into I_1^c in the case of $m_l = 0$ since $I_1^c = -I_2^c$. The integrated polarization fraction is given as

$$f_L \equiv \frac{\Gamma_0}{\Gamma} = \frac{\int dq^2 \frac{d\Gamma_0}{dq^2}}{\int dq^2 \frac{d\Gamma}{dq^2}}. \tag{19}$$

D. Forward-backward asymmetry

The differential forward-backward asymmetry of $\bar{B} \to \bar{K}_2^* l^+ l^-$ is defined by

$$\frac{dA_{\rm FB}}{dq^2} = \left[\int_0^1 - \int_{-1}^0\right] d\cos\theta_l \frac{d^2\Gamma}{dq^2 d\cos\theta_l} = \frac{3}{4}I_6, \tag{20}$$

while the normalized differential FBA is given by

$$\overline{\frac{dA_{\rm FB}}{dq^2}} = \frac{\frac{dA_{\rm FB}}{dq^2}}{\frac{d\Gamma}{dq^2}} = \frac{3I_6}{3I_1^c + 6I_1^s - I_2^c - 2I_2^s}. \tag{21}$$

In the massless limit, we have

$$\begin{aligned}\frac{dA_{\rm FB}}{dq^2} = \frac{\lambda}{8m_B^2 m_{K_2^*}^2}\frac{\lambda q^2 G_F^2 \alpha_{\rm em}^2}{512\pi^5 m_B^3}|V_{tb}V_{ts}^*|^2 \,{\rm Re}\Big[& C_9 C_{10} A_1 V \\ & + C_{10}(C_{7L} + C_{7R})\frac{m_b(m_B + m_{K_2^*})}{q^2}A_1 T_1 \\ & + C_{10}(C_{7L} - C_{7R})\frac{m_b(m_B - m_{K_2^*})}{q^2}T_2 V\Big].\end{aligned} \tag{22}$$

In the SM, where C_{7R} is small, the zero-crossing point s_0 of the FBAs is determined by the equation

$$\begin{aligned} & C_9 A_1(s_0)V(s_0) + C_{7L}\frac{m_b(m_B + m_{K_2^*})}{s_0}A_1(s_0)T_1(s_0) \\ & + C_{7L}\frac{m_b(m_B - m_{K_2^*})}{s_0}T_2(s_0)V(s_0) = 0.\end{aligned} \tag{23}$$

E. Spin amplitudes and transverse asymmetries

Using the above helicity/spin amplitudes, it is also possible to construct several useful quantities which are ratios of different amplitudes. The following ones, widely studied in the $B \to K^*$ case, are stable against the uncertainties from hadronic form factors,

$$\begin{aligned} A_T^{(1)} &= \frac{\Gamma_- - \Gamma_+}{\Gamma_- + \Gamma_+} = \frac{-2\,{\rm Re}(A_\parallel A_\perp^*)}{|A_\perp|^2 + |A_\parallel|^2}, \\ A_T^{(2)} &= \frac{|A_\perp|^2 - |A_\parallel|^2}{|A_\perp|^2 + |A_\parallel|^2}, \\ A_T^{(3)} &= \frac{|A_{L0}A_{L\parallel}^* + A_{R0}A_{R\parallel}^*|}{\sqrt{|A_0|^2|A_\perp|^2}}, \\ A_T^{(4)} &= \frac{|A_{L0}A_{L\perp}^* - A_{R0}A_{R\perp}^*|}{|A_{L0}A_{L\parallel}^* + A_{R0}A_{R\parallel}^*|}, \end{aligned} \tag{24}$$

with the notation

$$A_i A_j^* = A_{Li}A_{Lj}^* + A_{Ri}A_{Rj}^*. \tag{25}$$

Because of the hierarchy in the SM, $\Gamma_- \gg \Gamma_+$, $A_T^{(1)}$ is close to 1, and therefore its deviation from 1 is more useful to reflect the size of the NP effects.

IV. TWO NP MODELS

The $b \to s l^+ l^-$ has a small branching fraction since the SM has a lack of tree-level FCNCs. It is not necessarily the same in the extensions. In this section we will briefly give an overview of two NP models which allow tree-level FCNCs. Neither of these models, the vectorlike quark model and the family nonuniversal Z' model, introduces a new type of operator, but instead they both modify the Wilson coefficients C_9, C_{10}. To achieve this goal, they introduce an $SU(2)$ singlet down-type quark or a new gauge boson Z'.

A. Vectorlike quark model: Z-mediated FCNCs

In the vectorlike quark model, the new $SU(2)_L$ singlet down quarks D_L and D_R modify the Yukawa interaction sector

$$\mathcal{L}_Y = \bar{Q}_L Y_D H d_R + h_D \bar{Q}_L H D_R + m_D \bar{D}_L D_R + \text{H.c.}, \quad (26)$$

where the flavor indices have been suppressed. Q_L (H) is the $SU(2)$ quark (Higgs) doublet, Y_D and h_D are the Yukawa couplings, and m_D is the mass of the exotic quark before electroweak symmetry breaking. When the Higgs field acquires the vacuum expectation value (VEV), the mass matrix of the down-type quark becomes

$$m_d = \begin{pmatrix} Y_D^{ij} & | & h_D^i \\ - & - & - \\ 0 & | & m_D \end{pmatrix}, \quad (27)$$

which can be diagonalized by two unitary matrices,

$$m_d^{\text{dia}} = V_D^L m_d V_D^{R\dagger}. \quad (28)$$

The SM coupling of the Z boson to fermions is flavor blind, and the flavor in the process with the exchange of the Z boson is conserved at tree level. Unlikely although the right-handed sector in the VQM is the same as the SM, the new left-handed quark is an $SU(2)_L$ singlet, which carries the same hypercharge as right-handed particles. Therefore, the gauge interactions of left-handed down-type quarks with the Z boson are given by

$$\mathcal{L}_Z = \bar{Q}_L \frac{g}{\cos\theta_W}(I_3 - \sin^2\theta_W Q) \not{Z} Q_L + \bar{D}_L \frac{g}{\cos\theta_W}(-\sin^2\theta_W Q) \not{Z} D_L, \quad (29)$$

where g is the coupling constant of $SU(2)_L$, θ_W is the Weinberg angle, and $P_{R(L)} = (1 \pm \gamma_5)/2$. I_3 and Q are operators for the third component of the weak isospin and the electric charge, respectively.

Since the ratio ξ_D of the coupling constants deviates from unity, $\xi_D = -\sin^2\theta_W Q_D/(I_3^F - \sin^2\theta_W Q_F)$, tree-level FCNCs can be induced after the diagonalization of the down-type quarks. For instance, the interaction for b-s-Z in the VQM is given by

$$\mathcal{L}_{b\to s} = \frac{g c_L^s \lambda_{sb}}{\cos\theta_W} \bar{s} \gamma^\mu P_L b Z_\mu + \text{H.c.}, \quad (30)$$

where λ_{sb} is introduced as the new free parameter:

$$\lambda_{sb} = (\xi_D - 1)(V_D^L)_{sD}(V_D^L)^*_{bD} \equiv |\lambda_{sb}| \exp(i\theta_s).$$

Using Eq. (30), the effective Hamiltonian for $b \to s l^+ l^-$ mediated by the Z boson is found by

$$\mathcal{H}^Z_{b\to s l^+ l^-} = \frac{2G_F}{\sqrt{2}} \lambda_{sb} c_L^s (\bar{s} b)_{V-A} [c_L^\ell (\bar{\ell}\ell)_{V-A} + c_R^\ell (\bar{\ell}\ell)_{V+A}]. \quad (31)$$

The Wilson coefficients $C_{9,10}$ are modified accordingly,

$$C_9^{\text{VLQ}} = C_9^{\text{SM}} - \frac{4\pi}{\alpha_{\text{em}}} \frac{\lambda_{sb} c_L^s (c_L^\ell + c_R^\ell)}{V_{ts}^* V_{tb}}, \quad C_{10}^{\text{VLQ}} = C_{10}^{\text{SM}} + \frac{4\pi}{\alpha_{\text{em}}} \frac{\lambda_{sb} c_L^s (c_L^\ell - c_R^\ell)}{V_{ts}^* V_{tb}}. \quad (32)$$

Making use of the experimental data of $b \to s l^+ l^-$, our previous work [47] has placed a constraint on the new coupling constant

$$|\lambda_{sb}| < 1 \times 10^{-3}, \quad (33)$$

but its phase θ_s is less constrained. In the following, we shall see that the constraint can be improved by taking into account the experimental data of the exclusive process $B \to K^* l^+ l^-$.

B. Family nonuniversal Z′ model

The SM can be extended by including an additional $U(1)'$ symmetry, and the currents can be given in a proper gauge basis as follows:

$$J^\mu_{Z'} = g' \sum_i \bar{\psi}_i \gamma^\mu [\epsilon_i^{\psi_L} P_L + \epsilon_i^{\psi_R} P_R] \psi_i, \quad (34)$$

where i is the family index and ψ labels the fermions (up- or down-type quarks, or charged or neutral leptons). According to some string construction or grand unified theory models such as E_6, it is possible to have family nonuniversal Z' couplings, namely, even though $\epsilon_i^{L,R}$ are diagonal, the gauge couplings are not family universal. After rotating to the physical basis, FCNCs generally appear at tree level in both the left-handed and right-handed sectors. Explicitly,

$$B^{\psi_L} = V_{\psi_L} \epsilon^{\psi_L} V_{\psi_L}^\dagger, \qquad B^{\psi_R} = V_{\psi_R} \epsilon^{\psi_R} V_{\psi_R}^\dagger. \quad (35)$$

Moreover, these couplings may contain CP-violating phases beyond that of the SM.

The Lagrangian of $Z'\bar{b}s$ couplings is given as

$$\mathcal{L}^{Z'}_{\rm FCNC} = -g'(B^L_{sb}\bar{s}_L\gamma_\mu b_L + B^R_{sb}\bar{s}_R\gamma_\mu b_R)Z'^\mu + \text{H.c.} \quad (36)$$

It contributes to the $b \to s\ell^+\ell^-$ decay at tree level with the effective Hamiltonian

$$\mathcal{H}^{Z'}_{\rm eff} = \frac{8G_F}{\sqrt{2}}(\rho^L_{sb}\bar{s}_L\gamma_\mu b_L + \rho^R_{sb}\bar{s}_R\gamma_\mu b_R) \times (\rho^L_{ll}\bar{\ell}_L\gamma^\mu\ell_L + \rho^R_{ll}\bar{\ell}_R\gamma^\mu\ell_R), \quad (37)$$

where

$$\rho^{L,R}_{ff'} \equiv \frac{g'M_Z}{gM_{Z'}}B^{L,R}_{ff'} \quad (38)$$

with the coupling g associated with the $SU(2)_L$ group in the SM. In this paper we shall not take the renormalization group running effects due to these new contributions into consideration because they are expected to be small. Since the couplings are all unknown, one can see from Eq. (37) that there are many free parameters here. For the purpose of illustration and to avoid too many free parameters, we put the constraint that the FCNC couplings of the Z' and quarks only occur in the left-handed sector. Therefore, $\rho^R_{sb} = 0$, and the effects of the Z' FCNCs simply modify the Wilson coefficients C_9 and C_{10} in Eq. (A1). We denote these two modified Wilson coefficients by $C^{Z'}_9$ and $C^{Z'}_{10}$, respectively. More explicitly,

$$C^{Z'}_9 = C_9 - \frac{4\pi}{\alpha_{\rm em}}\frac{\rho^L_{sb}(\rho^L_{ll}+\rho^R_{ll})}{V_{tb}V^*_{ts}}, \qquad C^{Z'}_{10} = C_{10} + \frac{4\pi}{\alpha_{\rm em}}\frac{\rho^L_{sb}(\rho^L_{ll}-\rho^R_{ll})}{V_{tb}V^*_{ts}}. \quad (39)$$

Compared with the Wilson coefficients in the vectorlike quark model in Eq. (32), we can see that the Z' contributions in Eq. (39) have similar forms, and the correspondence lies in the coupling constants

$$\lambda_{sb}c^s_L \to \rho^L_{sb}, \qquad c^l_{L,R} \to \rho^{L,R}_{ll}. \quad (40)$$

However, the number of free parameters is increased from 2 to 4 since $c^l_{L,R}$ in the VQM is the same as in the SM.

V. PHENOMENOLOGICAL ANALYSIS

In this section, we will present our theoretical results in the SM, give an update of the constraints in the above two NP models, and investigate their effects on $B \to K^*_2\mu^+\mu^-$ and $B_s \to f'_2\mu^+\mu^-$. For convenience, branching ratios of K^*_2 and f'_2 decays into $K\pi$ and $K\bar{K}$ will not be taken into account in the numerical analysis.

A. SM predictions

With the $B \to K^*_2$ form factors computed in the PQCD approach [27], the BR, zero-crossing point of FBAs and polarization fractions are predicted as

$$\begin{aligned}
\mathcal{B}(B \to K^*_2\mu^+\mu^-) &= (2.5^{+1.6}_{-1.1}) \times 10^{-7},\\
f_L(B \to K^*_2\mu^+\mu^-) &= (66.6 \pm 0.4)\%,\\
s_0(B \to K^*_2\mu^+\mu^-) &= (3.49 \pm 0.04)\ \text{GeV}^2,\\
\mathcal{B}(B \to K^*_2\tau^+\tau^-) &= (9.6^{+6.2}_{-4.5}) \times 10^{-10},\\
f_L(B \to K^*_2\tau^+\tau^-) &= (57.2 \pm 0.7)\%.
\end{aligned} \quad (41)$$

The errors are from the form factors, namely, from the B meson wave functions and the PQCD systematic parameters. Most of the uncertainties from form factors will cancel in the polarization fractions and the zero-crossing point s_0. Similarly, results for $B_s \to f_2 l^+ l^-$ are given as

$$\begin{aligned}
\mathcal{B}(B_s \to f'_2\mu^+\mu^-) &= (1.8^{+1.1}_{-0.7}) \times 10^{-7},\\
f_L(B_s \to f'_2\mu^+\mu^-) &= (63.2 \pm 0.7)\%,\\
s_0(B_s \to f'_2\mu^+\mu^-) &= (3.53 \pm 0.03)\ \text{GeV}^2,\\
\mathcal{B}(B_s \to f'_2\tau^+\tau^-) &= (5.8^{+3.7}_{-2.1}) \times 10^{-10},\\
f_L(B_s \to f'_2\tau^+\tau^-) &= (53.9 \pm 0.4)\%.
\end{aligned} \quad (42)$$

We also show the q^2 dependence of their differential branching ratios (in units of 10^{-7}) in Fig. 2.

Charm-loop effects, due to the large Wilson coefficient and the large CKM matrix element, might introduce important results. In a very recent work [20], the authors have adopted QCD sum rules to investigate both factorizable diagrams and nonfactorizable diagrams. Their results up to the region $q^2 = m^2_{J/\psi}$ are parametrized in the following form,

$$\Delta C^{(i)B\to K^*}_9(q^2) = \frac{r^{(i)}_1(1-\frac{\bar{q}^2}{q^2}) + \Delta C^{(i)}_9(\bar{q}^2)\frac{\bar{q}^2}{q^2}}{1 + r^{(i)}_2\frac{\bar{q}^2-q^2}{m^2_{J/\psi}}}, \quad (43)$$

where the three results correspond to different Lorentz structures: $i = 1, 2, 3$ for terms containing V, A_1, and A_2, respectively. The numerical results are quoted as follows

$$\begin{aligned}
&\Delta C^{(1)}_9(\bar{q}^2) = 0.72^{+0.57}_{-0.37}, \quad r^{(1)}_1 = 0.10, \quad r^{(1)}_2 = 1.13,\\
&\Delta C^{(2)}_9(\bar{q}^2) = 0.76^{+0.70}_{-0.41}, \quad r^{(2)}_1 = 0.09, \quad r^{(2)}_2 = 1.12,\\
&\Delta C^{(3)}_9(\bar{q}^2) = 1.11^{+1.14}_{-0.70}, \quad r^{(3)}_1 = 0.06, \quad r^{(3)}_2 = 1.05.
\end{aligned} \quad (44)$$

It should be pointed out that not all charm-loop effects in $B \to K^*_2 l^+ l^-$ are the same as the ones in $B \to K^* l^+ l^-$. Among various diagrams, the factorizable contributions, which can be simply incorporated into C_9 given in Eq. (A3), are the same. The nonfactorizable ones are more subtle. In particular, the LCSR with B-meson distribution amplitudes are adopted in Ref. [20], in which intermediate states like K^* are picked up as the ground state. The generalization is not straightforward to the case of K^*_2 since in this approach states below K^*_2 may contribute in a substantial manner. However, in another viewpoint, i.e. the

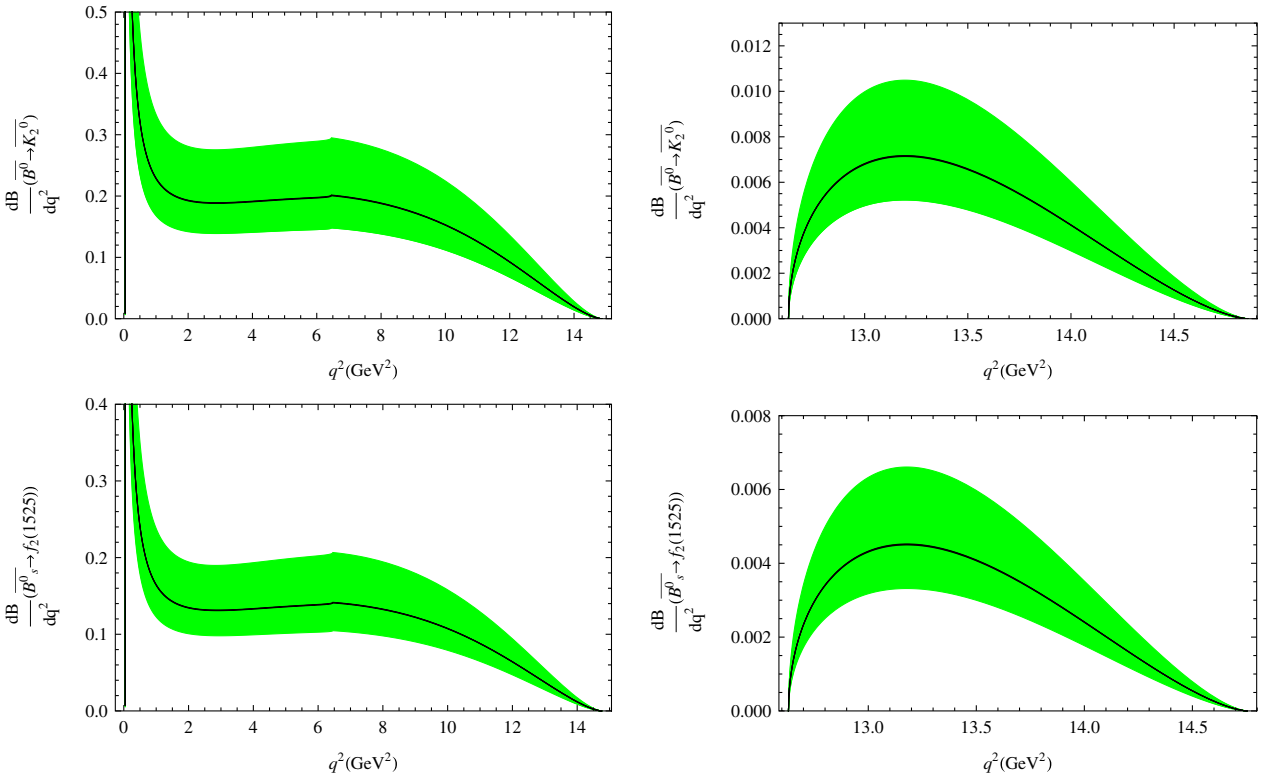

FIG. 2 (color online). Differential branching ratios of $B \to K_2^* l^+ l^-$ (upper panels) and $B_s \to f_2' l^+ l^-$ (lower panels) (in units of 10^{-7}). The left panel is for $l = \mu$ and the right panel is for $l = \tau$.

conventional LCSR, they may be related. In our previous work we have shown that the light-cone distribution amplitude of K_2^* is similar to K^* in the dominant region of the PQCD approach. If it were also the same in the conventional LCSR, one may expect that the charm-loop effects in the processes under scrutiny have similar behaviors as the ones in $B \to K^* l^+ l^-$. Therefore, as the first step to proceed, we will use their results to estimate the sensitivity in the following analysis, and to be conservative, we use

$$\Delta C_9^{(i)B\to K_2^*}(\bar{q}^2) = (1 \pm 1)\Delta C_9^{(i)B\to K^*}(q^2) \tag{45}$$

in the region of 1 $\mathrm{GeV}^2 < q^2 < 6$ GeV^2. The central values for q^2-dependent parameters will be used for simplicity, and in this procedure, the factorizable corrections to C_9 given in Eq. (A3) should be set to 0 to avoid double counting.

With the above strategy, our theoretical predictions are changed to

$$\begin{aligned} f_L(B \to K_2^* \mu^+ \mu^-) &= (66.6^{+1.4}_{-0.7})\%, \\ s_0(B \to K_2^* \mu^+ \mu^-) &= (3.49^{+0.19}_{-0.39})\ \mathrm{GeV}^2, \\ f_L(B_s \to f_2' \mu^+ \mu^-) &= (63.2^{+1.5}_{-0.9})\%, \\ s_0(B_s \to f_2' \mu^+ \mu^-) &= (3.53^{+0.19}_{-0.39})\ \mathrm{GeV}^2. \end{aligned} \tag{46}$$

The uncertainties in the zero-crossing point of the FBAs are enlarged to 0.4 GeV^2. We also show the q^2 dependence of the differential polarization in Fig. 3 and the normalized forward-backward asymmetries in Fig. 4.

In a parallel way, the BR of $B \to K_2^* l^+ l^-$ can also be estimated by making use of the data of radiative $B \to K^*(K_2^*)\gamma$ decays [48],

$$\begin{aligned} \mathcal{B}(\bar{B}^0 \to K_2^* \gamma) &= (12.4 \pm 2.4) \times 10^{-6}, \\ \mathcal{B}(\bar{B}^0 \to K^* \gamma) &= (43.3 \pm 1.5) \times 10^{-6}. \end{aligned} \tag{47}$$

The ratio of the above BRs, $R \equiv \frac{\mathcal{B}(K_2^*)}{\mathcal{B}(K^*)} = 0.29 \pm 0.06$, and the measured data of $B \to K^* l^+ l^-$ shown in Table II give the implication

$$\mathcal{B}_{\mathrm{exp}}(B^0 \to K_2^{*0} l^+ l^-) = (3.1 \pm 0.7) \times 10^{-7}, \tag{48}$$

which is remarkably consistent with our theoretical predictions within uncertainties.

When the large energy symmetry is exploited, the seven $B \to K_2^*$ form factors can be reduced into two independent ones, $\zeta_\perp$ and $\zeta_\parallel$. Based on these nontrivial relations, Ref. [25] has used the experimental data of $B \to K_2^* \gamma$ to extract $\zeta_\perp$. With the assumption of a similar size for $\zeta_\parallel$, the authors also estimated the branching ratio and forward-backward asymmetries of $B \to K_2^* l^+ l^-$. Explicitly, they have employed

$$\zeta_\perp = 0.27 \pm 0.03^{+0.00}_{-0.01}, \qquad 0.8\zeta_\perp < \zeta_\parallel < 1.2\zeta_\perp, \tag{49}$$

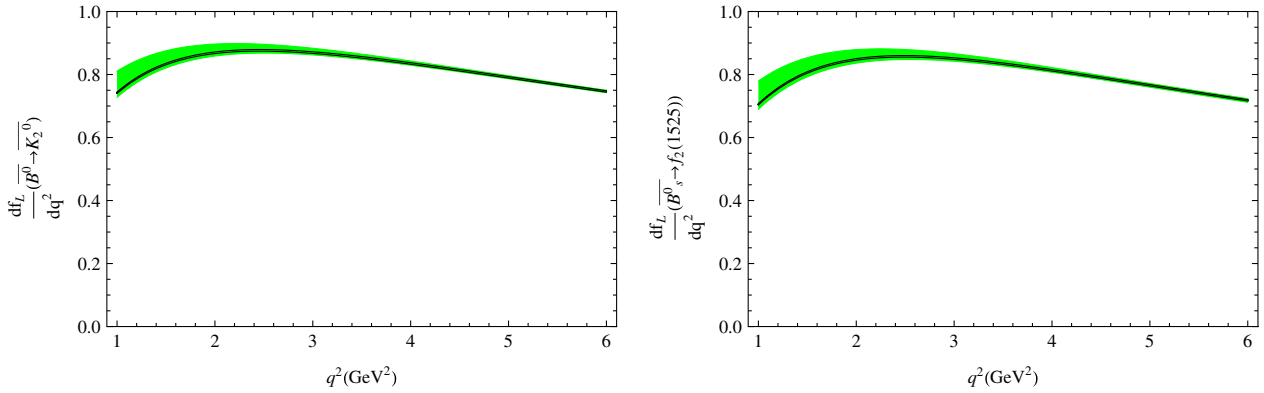

FIG. 3 (color online). Differential polarization fractions $\frac{df_L}{dq^2}$ of $B \to K_2^* l^+ l^-$ (left panel) and $B_s \to f_2 l^+ l^-$ (right panel).

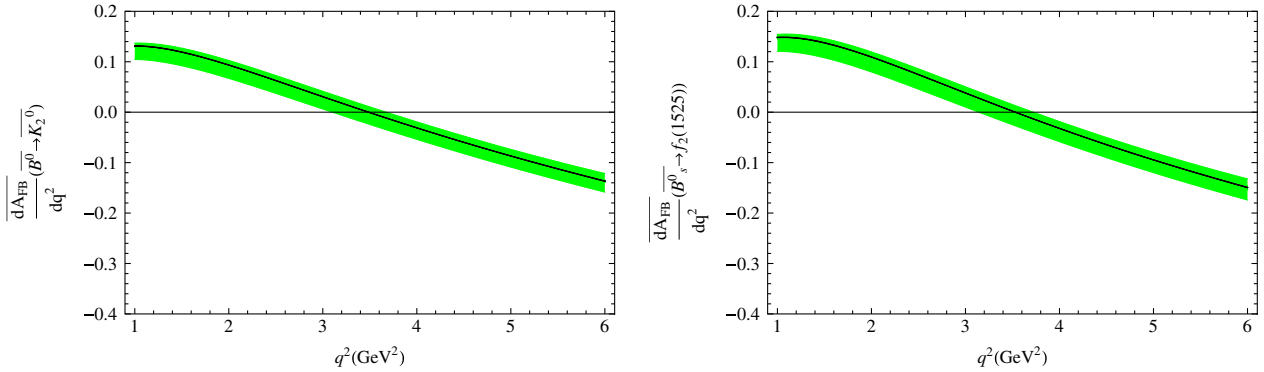

FIG. 4 (color online). Similar to Fig. 3 but for forward-backward asymmetries $\frac{dA_{FB}}{dq^2}$.

TABLE II. Experimental data used in the least-χ^2 fitting method.

$b \to c l \bar{\nu}$ [49] $(10.58 \pm 0.15) \times 10^{-2}$	$b \to s l^+ l^-$ [48] $(3.66^{+0.76}_{-0.77}) \times 10^{-6}$	$\bar{B}^0 \to K^* l^+ l^-$ [48] $(1.09^{+0.12}_{-0.11}) \times 10^{-6}$	
$q^2(\mathrm{GeV}^2)$	$\mathcal{B}(10^{-7})$	F_L	$-A_{FB}$[a]
[0, 2]	1.46 ± 0.41	0.29 ± 0.21	0.47 ± 0.32
[2, 4.3]	0.86 ± 0.32	0.71 ± 0.25	0.11 ± 0.37
[4.3, 8.68]	1.37 ± 0.61	0.64 ± 0.25	0.45 ± 0.26
[10.09, 12.86]	2.24 ± 0.48	0.17 ± 0.17	0.43 ± 0.20
[14.18, 16]	1.05 ± 0.30	-0.15 ± 0.28	0.70 ± 0.24
>16	2.04 ± 0.31	0.12 ± 0.15	0.66 ± 0.16
[1, 6]	1.49 ± 0.47	0.67 ± 0.24	0.26 ± 0.31

[a]The different convention on θ_l introduces a minus sign to the forward-backward asymmetry.

which are comparable with our results [27],

$$\zeta_\perp = (0.29 \pm 0.09), \qquad \zeta_\parallel = (0.26 \pm 0.10). \tag{50}$$

As a consequence, the predicted results of the BR, forward-backward asymmetries, and polarizations are compatible with each other.

Our results for the angular coefficients, $\bar{I}_i = I_i / \frac{d\Gamma}{dq^2}$, are depicted in Fig. 5 for $B \to K_2^* \mu^+ \mu^-$ and in Fig. 6 for $B_s \to f_2' \mu^+ \mu^-$. Since the predictions for $\bar{I}_7$, $\bar{I}_8$, $\bar{I}_9$ in the SM are typically smaller than 0.03, we shall not show them. The corresponding transversity asymmetries are shown in Figs. 7 and 8, respectively. One particular feature is that most of these results are stable against the large uncertainties from the form factors.

For experimental purposes, it is valuable to estimate the minimum size of the averaged value of an angular distribution coefficient so that it can be measured in experiment. To establish any generic asymmetry with the averaged value $\langle A \rangle$ of a particular decay at the $n\sigma$ level, events of

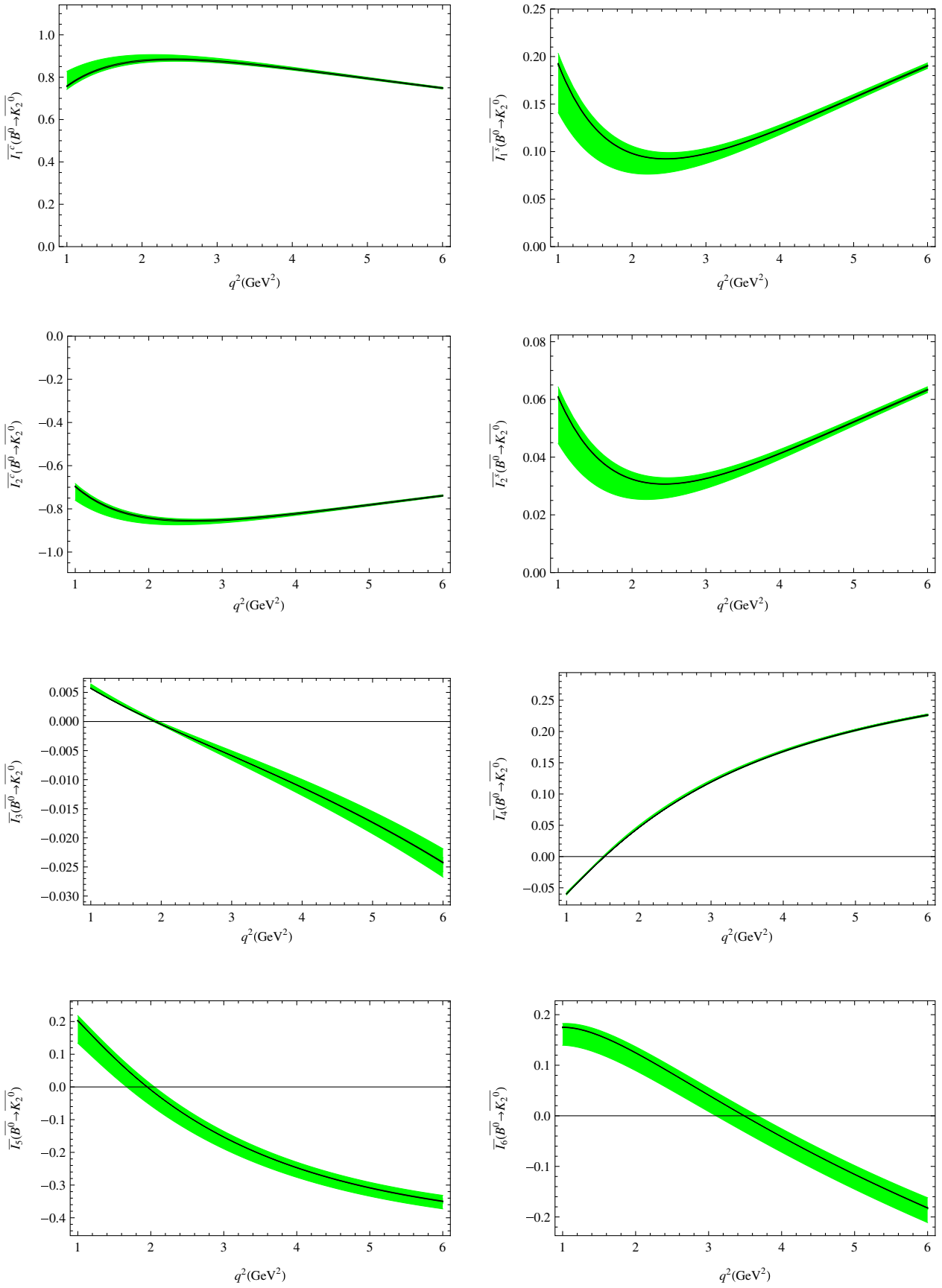

FIG. 5 (color online). Angular coefficients $\bar{I}_i$ for $B \to K_2^* \mu^+ \mu^-$.

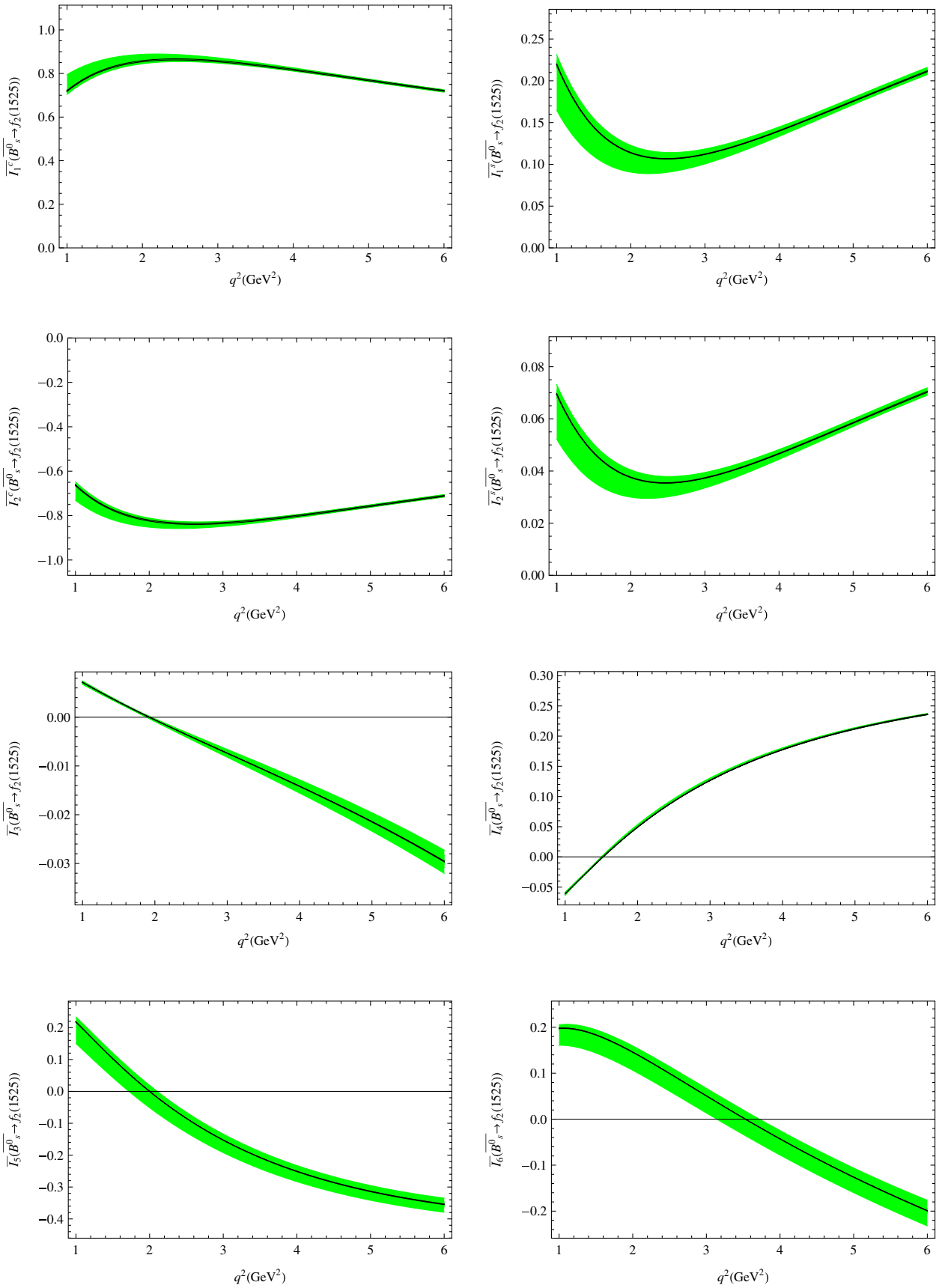

FIG. 6 (color online). Similar to Fig. 5 but for $B_s \to f_2 \mu^+ \mu^-$.

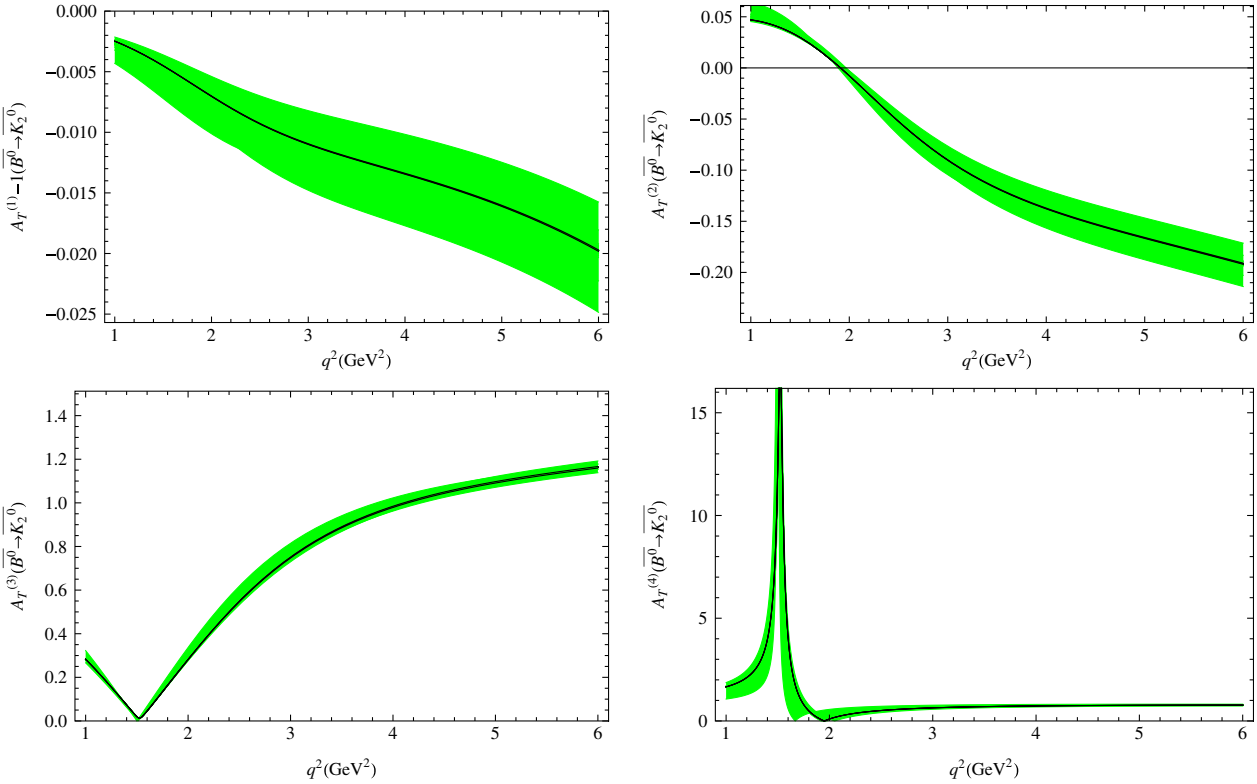

FIG. 7 (color online). Spin amplitudes and transversity asymmetries of $B \to K_2^* \mu^+ \mu^-$.

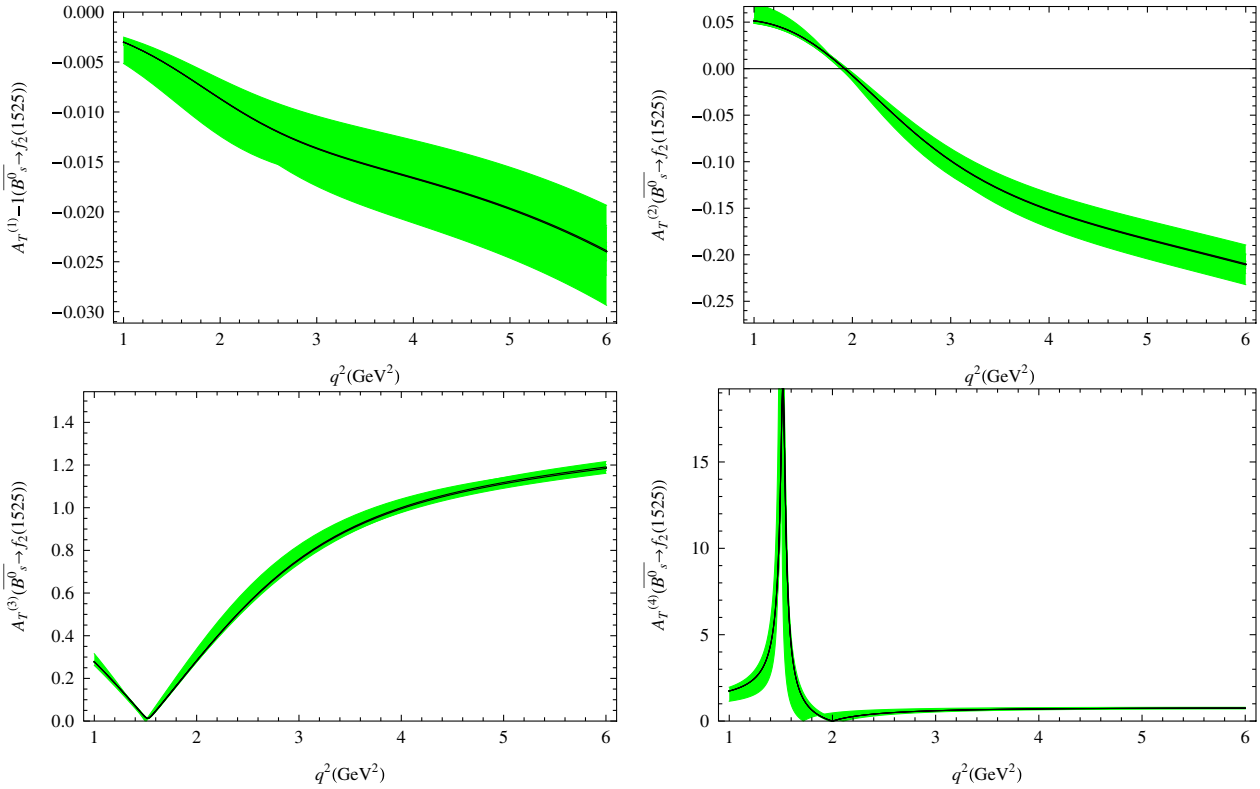

FIG. 8 (color online). Similar to Fig. 7 but for $B_s \to f_2 \mu^+ \mu^-$.

the number $N = n^2/(\langle A\rangle)^2$ should be accumulated. For instance, on the LHCb there are 6200 events for the $B \to K^* l^+ l^-$ process per nominal running year [4]. Incorporating all differences between K_2^* and K^*, we may expect roughly 1000 events of $B \to K_2^*(\to K\pi) l^+ l^-$. Therefore, if one wants to observe an asymmetry at the $n\sigma$ level, its averaged value should be larger than $\langle A\rangle_{\min} = \sqrt{\frac{n^2}{1000}} \simeq 0.03n$.

Before closing this subsection, it is necessary to point out that the above estimation might be too optimistic. In the first few running years of LHCb, the central energy in the pp collision may not reach 14 TeV and its luminosity will be below 2 fb^{-1}. Thus, in the first stage, not enough data are available for a precise determination of some angular coefficients. Nevertheless, this will not affect our analysis of branching fractions and many angular coefficients.

B. Constraints on NP parameters and the NP effects on $B \to K_2^* \mu^+ \mu^-$

In this subsection we will first update the constraints of the free parameters in the two NP models above, and particularly, we use the experimental data of $b \to s l^+ l^-$ and $B \to K^* l^+ l^-$. The decay width of the inclusive process $b \to s l^+ l^-$ is given as [50]

$$\frac{d\Gamma(b \to s\ell^+\ell^-)}{d\hat{s}} = \Gamma(b \to ce\bar{\nu}_e)\frac{|V_{ts}^*|^2}{|V_{cb}|^2}\frac{\alpha_{\rm em}^2}{4\pi^2}\frac{(1-\hat{s})^2}{f(\hat{m}_c)k(\hat{m}_c)}\left[(1+2\hat{s})(|C_9|^2+|C_{10}|^2)+4\left(1+\frac{2}{\hat{s}}\right)|C_7|^2+12C_7\,{\rm Re}C_9\right],$$
$$f(z) = 1-8z^2+8z^6-z^8-24z^4\ln z,$$
$$k(z) = 1-\frac{2\alpha_s}{3\pi}\left[\left(\pi^2-\frac{31}{4}\right)(1-z)^2+\frac{3}{2}\right], \tag{51}$$

where $\hat{s} = q^2/m_b^2$, and $\Gamma(b \to ce\bar{\nu}_e)$ is used to cancel the uncertainties from the CKM matrix elements and the factor m_b^5. For $B \to K^* l^+ l^-$, the FBAs, polarizations, and BR have been measured in different kinematic bins [2]. The other relevant experimental data collected in Table II are from Refs. [48,49].

We will adopt a least-χ^2 fitting method to constrain the free parameters, in which the χ^2 is defined by

$$\chi_i^2 = \frac{(B_i^{\rm the} - B_i^{\rm exp})^2}{(B_i^{\rm err})^2}, \tag{52}$$

where B_i denotes one generic quantity among the physical observables. The $B_i^{\rm the}$, $B_i^{\rm exp}$, and $B_i^{\rm err}$ denote the theoretical prediction, the central value, and the 1-σ error of the experimental data, respectively. The total χ^2 is obtained by adding the individual ones. It is necessary to point out that although the errors in the experiment may correlate, for instance the measurement of $\mathcal{B}$, f_L, and $A_{\rm FB}$ proceed at the same time in the fitting of angular distributions [2], we have not taken into account their correlation in our theoretical results.

As shown in the previous section, these two NP models have the similarity that only $C_{9,10}$ are modified. One difference lies in the coupling with the leptons; the newly introduced down-type quark in the VQM will not modify the lepton sector and the coupling with leptons is SM-like. On the contrary, one new gauge boson is added in the Z' model and its coupling with leptons is completely unknown.

Embedded in the VQM, the two parameters, the real and imaginary parts of λ_{sb}, are found as

$$\begin{aligned} {\rm Re}\,\lambda_{sb} &= (0.07 \pm 0.04)\times 10^{-3}, \\ {\rm Im}\lambda_{sb} &= (0.09 \pm 0.23)\times 10^{-3}, \end{aligned} \tag{53}$$

from which we obtain $|\lambda_{sb}| < 0.3 \times 10^{-3}$, but the phase is less constrained again. The corresponding constraints on the Wilson coefficients are

$$|\Delta C_9| = |C_9 - C_9^{\rm SM}| < 0.2, \quad |\Delta C_{10}| = |C_{10} - C_{10}^{\rm SM}| < 2.8. \tag{54}$$

Our result for χ^2/d.o.f. in the fitting method is $49.3/(23-2)$.

Turning to the family nonuniversal Z' model in which the coupling between Z' and a lepton pair is unknown, the two Wilson coefficients C_9 and C_{10} can be chosen as independent parameters. Assuming ΔC_9 and ΔC_{10} as real, we find

$$\Delta C_9 = 0.88 \pm 0.75, \qquad \Delta C_{10} = 0.01 \pm 0.69, \tag{55}$$

with χ^2/d.o.f. $= 48.4/(23-2)$. Removal of the above assumption leads to

$$\begin{aligned} \Delta C_9 &= -0.81 \pm 1.22 + (3.05 \pm 0.92)i, \\ \Delta C_{10} &= 1.00 \pm 1.28 + (-3.16 \pm 0.94)i \end{aligned} \tag{56}$$

with χ^2/d.o.f. $= 45.6/(23-4)$. If the μ-lepton mass is neglected, the imaginary part of C_{10} will not appear in the expressions for the differential decay widths and the polarizations. Moreover, for the forward-backward asymmetry as shown in Eq. (22), the imaginary part of C_{10} contributes in the combination ${\rm Re}[C_9 C_{10}]$; thus, the inclusion of ${\rm Im}[C_{10}]$ will have little effect on the χ^2.

Combing the above results, we can see that the NP contributions in both cases satisfy

$$|\Delta C_9| < 3, \qquad |\Delta C_{10}| < 3. \tag{57}$$

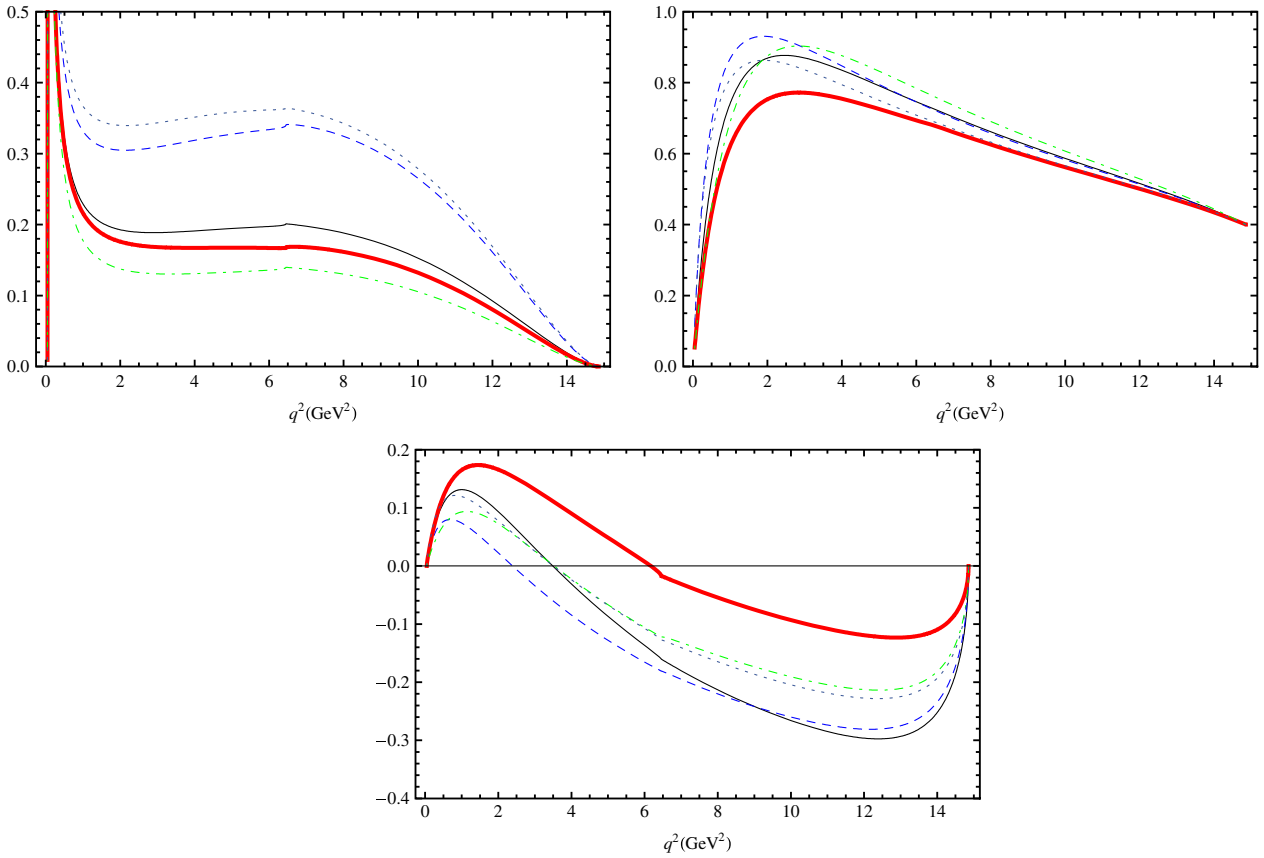

FIG. 9 (color online). The impact of the NP contributions on differential branching ratios (in units of 10^{-7}), polarization fractions, and normalized forward-backward asymmetry of $B \to K_2^* l^+ l^-$.

To illustrate, we choose $\Delta C_9 = 3e^{i\pi/4, i3\pi/4}$ and $\Delta C_{10} = 3e^{i\pi/4, i3\pi/4}$ as the reference points and give the plots for the branching ratios, FBAs, and the polarizations in Fig. 9. The solid (black) line denotes the SM result, while the dashed (blue) and thick (red) lines correspond to the modification of C_9. The dot-dashed (green) and dotted lines are obtained by modifying C_{10}. From the figure for A_{FB}, we can see that the zero-crossing point s_0 can be sizably changed, which can be tested at the LHC or can be further constrained.

One last process to explore is $B_s \to \mu^+ \mu^-$, of which the branching fraction is

$$\mathcal{B}(B_s \to \mu^+ \mu^-) = \tau_{B_s} \frac{G_F^2 \alpha_{\mathrm{em}}^2}{16\pi^3} |V_{ts}^* V_{tb}|^2 m_{B_s} f_{B_s}^2 m_\mu^2 |C_{10}|^2 \times \left(1 - \frac{4m_\mu^2}{m_{B_s}^2}\right)^{1/2}. \quad (58)$$

Using the same inputs as those in our computation of $B \to K_2^* l^+ l^-$, we have

$$\mathcal{B}(B_s \to \mu^+ \mu^-) = 3.50 \times 10^{-9} \left(\frac{f_{B_s}}{230\ \mathrm{MeV}}\right)^2 \left(\frac{|C_{10}|}{4.67}\right)^2. \quad (59)$$

Even if C_{10} is enhanced by a factor of 2, the above result is still consistent with the recent measurement [51]

$$\mathcal{B}(B_s \to \mu^+ \mu^-) < 5.1 \times 10^{-8}. \quad (60)$$

VI. SUMMARY

In this work we have explored $B \to K_2^*(\to K\pi) l^+ l^-$ (with $l = e,\ \mu,\ \tau$) decays and a similar mode $B_s \to f_2'(1525)(\to K^+ K^-) l^+ l^-$ in the standard model and two new physics scenarios: the vectorlike quark model and the family nonuniversal Z' model. Besides branching ratios, forward-backward asymmetries, and transversity amplitudes, we have also derived the differential angular distributions of this decay chain. The sizable production rates lead to a promising prospective to observe this channel in future experiments.

Using the experimental data of the inclusive $b \to s l^+ l^-$ and $B \to K^* l^+ l^-$, we have updated the constraints on the effective Wilson coefficients and/or free parameters in these two new physics scenarios. In the VQM, we find that the constraint on the coupling constant is improved by a factor of 3 compared with our previous work. Their impact on $B \to K_2^* l^+ l^-$ is elaborated and, in particular, the zero-crossing point for the forward-backward asymmetry in these NP scenarios can sizably deviate from the SM. These results will be tested at the LHC.

ACKNOWLEDGMENTS

This work is partly supported by the National Natural Science Foundation of China under Grants No. 10735080, No. 11075168, and No. 10625525, and by the National Basic Research Program of China (973) Grant No. 2010CB833000 (C. D. L.), the Brain Korea 21 Project (R. H. L.), and Alexander von Humboldt Stiftung (W. W.). We thank K. C. Yang for useful discussions on the coefficient $\mathcal{C}$ defined in Eq. (B11) in Appendix B. W. W. is grateful to Professor Ahmed Ali for valuable discussions, C. H. Chen for the collaboration and useful discussions on the vectorlike quark model, and Yuming Wang for useful discussions on charm-loop effects.

APPENDIX A: EFFECTIVE HAMILTONIAN

The effective Hamiltonian governing $b \to s l^+ l^-$ is given by

$$\mathcal{H}_{\rm eff} = -\frac{G_F}{\sqrt{2}} V_{tb} V_{ts}^* \sum_{i=1}^{10} C_i(\mu) O_i(\mu), \tag{A1}$$

where $V_{tb} = 0.999\,176$ and $V_{ts} = -0.039\,72$ [49] are the CKM matrix elements and $C_i(\mu)$ are Wilson coefficients for the effective operators O_i. In this paper, we will adopt the Wilson coefficients up to the leading logarithmic accuracy [50], and their values in the SM are listed in Table III. Since the NP scenarios considered in the present paper would not introduce any new operator, the SM operators will form a complete basis for our analysis,

$$\begin{aligned}
O_1 &= (\bar{s}_\alpha c_\alpha)_{V-A} (\bar{c}_\beta b_\beta)_{V-A}, \\
O_2 &= (\bar{s}_\alpha c_\beta)_{V-A} (\bar{c}_\beta b_\alpha)_{V-A}, \\
O_3 &= (\bar{s}_\alpha b_\alpha)_{V-A} \sum_q (\bar{q}_\beta q_\beta)_{V-A}, \\
O_4 &= (\bar{s}_\alpha b_\beta)_{V-A} \sum_q (\bar{q}_\beta q_\alpha)_{V-A}, \\
O_5 &= (\bar{s}_\alpha b_\alpha)_{V-A} \sum_q (\bar{q}_\beta q_\beta)_{V+A}, \\
O_6 &= (\bar{s}_\alpha b_\beta)_{V-A} \sum_q (\bar{q}_\beta q_\alpha)_{V+A}, \\
O_7 &= \frac{{\rm em}_b}{8\pi^2} \bar{s} \sigma^{\mu\nu} (1+\gamma_5) b F_{\mu\nu} + \frac{{\rm em}_s}{8\pi^2} \bar{s} \sigma^{\mu\nu} (1-\gamma_5) b F_{\mu\nu}, \\
O_9 &= \frac{\alpha_{\rm em}}{2\pi} (\bar{l} \gamma_\mu l) (\bar{s} \gamma^\mu (1-\gamma_5) b), \\
O_{10} &= \frac{\alpha_{\rm em}}{2\pi} (\bar{l} \gamma_\mu \gamma_5 l) (\bar{s} \gamma^\mu (1-\gamma_5) b).
\end{aligned} \tag{A2}$$

The left-handed and right-handed operators are $(\bar{q}_1 q_2)_{V-A} (\bar{q}_3 q_4)_{V\pm A} \equiv (\bar{q}_1 \gamma^\mu (1-\gamma_5) q_2)(\bar{q}_3 \gamma_\mu (1 \pm \gamma_5) q_4)$. $m_b = 4.8$ GeV and $m_s = 0.095$ GeV are b and s quark masses in the $\overline{\rm MS}$ scheme, and $\alpha_{\rm em} = 1/137$ is the fine-structure constant. The double Cabibbo suppressed terms, proportional to $V_{ub} V_{us}^*$, have been neglected.

At one-loop level accuracy, the matrix element of the $b \to s l^+ l^-$ transition receives loop contributions from O_1–O_6. Since the factorizable loop terms [52] can be incorporated into the Wilson coefficients C_7 and C_9, it is convenient to define the combinations $C_7^{\rm eff}$ and $C_9^{\rm eff}$ [52],

$$\begin{aligned}
C_7^{\rm eff} &= C_7 - C_5/3 - C_6, \\
C_9^{\rm eff}(q^2) &= C_9(\mu) + h(\hat{m}_c, \hat{s}) C_0 - \tfrac{1}{2} h(1, \hat{s})(4C_3 + 4C_4 \\
&\quad + 3C_5 + C_6) - \tfrac{1}{2} h(0, \hat{s})(C_3 + 3C_4) \\
&\quad + \tfrac{2}{9}(3C_3 + C_4 + 3C_5 + C_6),
\end{aligned} \tag{A3}$$

with $\hat{s} = q^2/m_b^2$, $C_0 = C_1 + 3C_2 + 3C_3 + C_4 + 3C_5 + C_6$, and $\hat{m}_c = m_c/m_b$. The auxiliary functions used above are

$$\begin{aligned}
h(z, \hat{s}) &= -\frac{8}{9} \ln \frac{m_b}{\mu} - \frac{8}{9} \ln z + \frac{8}{27} + \frac{4}{9} x - \frac{2}{9}(2+x) \\
&\quad \times |1-x|^{1/2} \begin{cases} \ln \left| \frac{\sqrt{1-x}+1}{\sqrt{1-x}-1} \right| - i\pi & \text{for } x \equiv \frac{4z^2}{\hat{s}} < 1 \\ 2 \arctan \frac{1}{\sqrt{x-1}} & \text{for } x \equiv \frac{4z^2}{\hat{s}} > 1, \end{cases} \\
h(0, \hat{s}) &= -\frac{8}{9} \ln \frac{m_b}{\mu} - \frac{4}{9} \ln \hat{s} + \frac{8}{27} + \frac{4}{9} i\pi.
\end{aligned} \tag{A4}$$

In the following, we shall also drop the superscripts for $C_9^{\rm eff}$ and $C_7^{\rm eff}$ for convenience.

On the hadron level, resonant states, such as vector charmonia generated from the $b \to c\bar{c}s$, may annihilate into a lepton pair. Therefore, they will also contribute in a long-distance manner [53–55]. But these contributions can be subtracted with a kinematic cutoff in experiment. Moreover, our following analysis of differential distributions will be mainly dedicated to the region of $1\ {\rm GeV}^2 < q^2 < 6\ {\rm GeV}^2$, also excluding contributions from the charmonia.

APPENDIX B: HELICITY AMPLITUDES

Within a graphic picture, $B \to K_2^*(\to K\pi) l^+ l^-$ proceeds in three steps: the B meson first decays into an on-shell strange meson plus a pair of leptons, the K_2^* meson propagates, and then it strongly decays into $K\pi$. To evaluate the

TABLE III. The values of the Wilson coefficients $C_i(m_b)$ in the leading logarithmic approximation, with $m_W = 80.4$ GeV, $\mu = m_{b,\rm pole}$ [50].

C_1	C_2	C_3	C_4	C_5	C_6	$C_7^{\rm eff}$	C_9	C_{10}
1.107	−0.248	−0.011	−0.026	−0.007	−0.031	−0.313	4.344	−4.669

decay width of multibody decays, we shall adopt the helicity amplitude, which mainly uses

$$g_{\mu\nu} = -\sum_{\lambda} \epsilon_{\mu}(\lambda)\epsilon^{*}_{\nu}(\lambda) + \frac{q_\mu q_\nu}{q^2}. \tag{B1}$$

ϵ is the polarization vector with the momentum q, and λ denotes the three kinds of polarizations. The last term can be formally identified as a timelike polarization $\epsilon_\mu(t) = \frac{q_\mu}{\sqrt{q^2}}$, and thus the metric tensor $g_{\mu\nu}$ can then be understood as summations of the four polarizations. For the purpose of illustration, we will first evaluate the decay amplitude of $B \to K_2^* l^+ l^-$. In the SM, the lepton pair in the final state is produced via an off-shell photon, a Z boson, or some hadronic vector mesons. These states may have different couplings but they share many commonalities: the Lorentz structure for the vertex of the lepton pair is either $V - A$ or $V + A$ or some combination of them. Therefore, the decay amplitudes of $\bar{B} \to \bar{K}_2^* l^+ l^-$ can be rewritten as

$$\mathcal{A}(\bar{B} \to \bar{K}_2^* l^+ l^-) = \mathcal{L}^{\mu}(L)\mathcal{H}_{\mu}(L) + \mathcal{L}^{\mu}(R)\mathcal{H}_{\mu}(R), \tag{B2}$$

in which $\mathcal{L}_\mu(L)$, $\mathcal{L}_\mu(R)$ are the lepton pair spinor products:

$$\mathcal{L}_{\mu}(L) = \bar{l}\gamma_\mu(1-\gamma_5)l, \qquad \mathcal{L}_\mu(R) = \bar{l}\gamma_\mu(1+\gamma_5)l, \tag{B3}$$

while $\mathcal{H}$ incorporates the remaining $B \to K_2^*$ part. In the case of massless leptons, left-handed and right-handed sectors decouple, which will greatly simplify the analysis. The identity in Eq. (B1) results in a factorization of decay amplitudes,

$$\mathcal{A}(\bar{B} \to \bar{K}_2^* l^+ l^-) = \mathcal{L}_\mu(L)\mathcal{H}_\nu(L)g^{\mu\nu} + \mathcal{L}_\mu(R)\mathcal{H}_\nu(R)g^{\mu\nu} = -\sum_\lambda \mathcal{L}_{L\lambda}\mathcal{H}_{L\lambda} - \sum_\lambda \mathcal{L}_{R\lambda}\mathcal{H}_{R\lambda}, \tag{B4}$$

where q^μ is the momentum of the lepton pair and $\mathcal{L}_{L\lambda} = \mathcal{L}^\mu(L)\epsilon_\mu(\lambda)$ and $\mathcal{L}_{R\lambda} = \mathcal{L}^\mu(R)\epsilon_\mu(\lambda)$ denote Lorentz invariant amplitudes for the lepton part. It is also similar for the Lorentz invariant hadronic amplitudes: $\mathcal{H}_{L\lambda} = \mathcal{H}^\mu(L)\epsilon^*_\mu(\lambda)$ and $\mathcal{H}_{R\lambda} = \mathcal{H}^\mu(R)\epsilon^*_\mu(\lambda)$. The timelike polarization gives vanishing contributions in the case of $m_l = 0$ for $l = e$, μ; using the equation of motion, this term is proportional to the lepton mass.

An advantage of the helicity amplitudes is that both hadronic amplitudes and leptonic amplitudes are Lorentz invariant. Such a good property allows one to choose different frames in the evaluation. For instance, leptonic amplitudes are evaluated in the lepton pair central mass frame, while hadronic B decay amplitudes are directly obtained in the B rest frame. Since K_2^* and K^* have several important similarities, $B \to K_2^* l^+ l^-$ differential decay widths can be simply obtained from the ones of $B \to K^* l^+ l^-$ in a comparative manner.

(i) Longitudinal and transverse B decay amplitudes are obtained by multiplying the factors $\frac{\sqrt{\lambda}}{\sqrt{8}m_B m_{K_2^*}}$ and $\frac{\sqrt{\lambda}}{\sqrt{6}m_B m_{K_2^*}}$, respectively. The function λ is the magnitude of the K_2^* momentum in the B meson rest frame: $\lambda \equiv \lambda(m_B^2, m_{K_2^*}^2, q^2) = 2m_B|\vec{p}_{K_2^*}|$ and $\lambda(a^2, b^2, c^2) = (a^2 - b^2 - c^2)^2 - 4b^2c^2$. This replacement is a result of the fact that the polarization vector ϵ is replaced by ϵ_T in the form factor definitions. Explicitly, these hadronic amplitudes are

$$\begin{aligned}
H_{L0} &= N\frac{\sqrt{\lambda}}{\sqrt{8}m_B m_{K_2^*}}\frac{1}{2m_{K_2^*}\sqrt{q^2}}\Big[(C_9 - C_{10})\Big[(m_B^2 - m_{K_2^*}^2 - q^2)(m_B + m_{K_2^*})A_1 - \frac{\lambda}{m_B + m_{K_2^*}}A_2\Big] \\
&\quad + 2m_b(C_{7L} - C_{7R})\Big[(m_B^2 + 3m_{K_2^*}^2 - q^2)T_2 - \frac{\lambda}{m_B^2 - m_{K_2^*}^2}T_3\Big]\Big], \\
H_{L\pm} &= N\frac{\sqrt{\lambda}}{\sqrt{6}m_B m_{K_2^*}}\Big[(C_9 - C_{10})\Big[(m_B + m_{K_2^*})A_1 \mp \frac{\sqrt{\lambda}}{m_B + m_{K_2^*}}V\Big] - \frac{2m_b(C_{7L} + C_{7R})}{q^2}(\pm\sqrt{\lambda}T_1) \\
&\quad + \frac{2m_b(C_{7L} - C_{7R})}{q^2}(m_B^2 - m_{K_2^*}^2)T_2\Big], \\
H_{Lt} &= N\frac{\sqrt{\lambda}}{\sqrt{8}m_B m_T}(C_9 - C_{10})\frac{\sqrt{\lambda}}{\sqrt{q^2}}A_0, \\
H_{Ri} &= H_{Li}|_{C_{10}\to -C_{10}}
\end{aligned} \tag{B5}$$

with $N = -i\frac{G_F}{4\sqrt{2}}\frac{\alpha_{\rm em}}{\pi}V_{tb}V_{ts}^*$.

(ii) In the propagation of the intermediate strange meson, the width effect of K_2^* could be more important since $\Gamma_{K_2^*} \sim 100$ MeV $> \Gamma_{K^*} \sim 50$ MeV [49]. Nevertheless, since the K_2^* width is only larger than that of K^* by a factor of 2, the narrow-width approximation, which has been well used in the case of K^*, might also work for K_2^*. In this sense, there is

no difference except that the $\mathcal{B}(K^* \to K\pi)$ is replaced by $\mathcal{B}(K_2^* \to K\pi)$.

(iii) Incorporation of the $K_2^* \to K\pi$ decay gives the complete results for the differential decay distribution of $B \to K_2^*(\to K\pi)l^+l^-$. Angular distributions of K_2^* and K^* strong decays are described by spherical harmonic functions: $Y_1^i(\theta, \phi)$ for K^* and $Y_2^i(\theta, \phi)$ for K_2^*. In particular, we find the relations

$$\sqrt{\frac{3}{4\pi}}\cos(\theta_K) \equiv C(K^*) \to \sqrt{\frac{5}{16\pi}}(3\cos^2\theta_K - 1) \equiv C(K_2^*),$$
$$\sqrt{\frac{3}{8\pi}}\sin(\theta_K) \equiv S(K^*) \to \sqrt{\frac{15}{32\pi}}\sin(2\theta_K) \equiv S(K_2^*). \tag{B6}$$

Our formulas for the branching fractions and forward-backward asymmetries are shown to be compatible with the ones in Ref. [25] through the following relations:

$$A_{L0} = N_{K_2^*}\alpha_L m_B^3 \frac{1}{2m_{K_2^*}\sqrt{q^2}}(-(1 - \hat{m}_{K_2^*}^2 - \hat{q}^2)\mathcal{F} + \hat{\lambda}\mathcal{G} + (1 - \hat{m}_{K_2^*}^2 - \hat{q}^2)\mathcal{B} - \hat{\lambda}\mathcal{C}), \tag{B7}$$

$$A_{L\perp} = -\frac{\sqrt{2\lambda}N_{K_2^*}\beta_T}{2m_B}(\mathcal{A} - \mathcal{E}), \tag{B8}$$

$$A_{L\parallel} = \frac{\sqrt{2\lambda}N_{K_2^*}\beta_T}{2m_B}(\mathcal{B} - \mathcal{F}), \tag{B9}$$

$$A_t = \frac{N_{K_2^*}\alpha_L}{\hat{m}_{K_2^*}}\frac{\sqrt{\lambda}}{\sqrt{q^2}}[\mathcal{F} - (1 - \hat{m}_{K_2^*}^2\mathcal{G} - \hat{q}^2\mathcal{H}], \tag{B10}$$

where the coefficients $\mathcal{A}$, $\mathcal{B}$, $\mathcal{E}$, $\mathcal{F}$, $\mathcal{G}$, $\mathcal{H}$ are defined in Eqs. (49, 50, 53, 54) in Ref. [25], but the coefficient $\mathcal{C}$ in Eq. (51) contains a typo and should be

$$\mathcal{C} = \frac{1}{1 - \hat{m}_{K_2^*}^2}\Big[(1 - \hat{m}_{K_2^*})c_9^{\text{eff}}(\hat{s})A_2^{K_2^*}(s) + 2\hat{m}_b c_7^{\text{eff}}\Big(T_3^{K_2^*}(s) + \frac{1 - \hat{m}_{K_2^*}^2}{\hat{s}}T_2^{K_2^*}(s)\Big)\Big]. \tag{B11}$$

The dimensionless constants are given as $\hat{\lambda} = \lambda/m_B^4$, $\hat{m}_{K_2^*} = m_{K_2^*}/m_B$, $\hat{m}_b = m_b/m_B$, and $\hat{q}^2 = q^2/m_B^2$, as well as $\alpha_L = \sqrt{2/3}$ and $\beta_T = 1/\sqrt{2}$.

[1] B. Aubert *et al.* (*BABAR* Collaboration), Phys. Rev. Lett. **102**, 091803 (2009).
[2] J. T. Wei *et al.* (Belle Collaboration), Phys. Rev. Lett. **103**, 171801 (2009).
[3] T. Aaltonen *et al.* (CDF Collaboration), Phys. Rev. D **79**, 011104 (2009).
[4] B. Adeva *et al.* (LHCb Collaboration), arXiv:0912.4179; M. Patel and H. Skottowe, Report No. LHCb-2009-009.
[5] R. L. Gac (LHCb Collaboration), arXiv:1009.5902.
[6] B. O'Leary *et al.* (SuperB Collaboration), arXiv:1008.1541.
[7] A. Ali, P. Ball, L. T. Handoko *et al.*, Phys. Rev. D **61**, 074024 (2000).
[8] C. S. Kim, Y. G. Kim, C. D. Lu, and T. Morozumi, Phys. Rev. D **62**, 034013 (2000).
[9] M. Beneke, T. Feldmann, and D. Seidel, Nucl. Phys. **B612**, 25 (2001).
[10] C. H. Chen and C. Q. Geng, Nucl. Phys. **B636**, 338 (2002).
[11] F. Kruger and J. Matias, Phys. Rev. D **71**, 094009 (2005).
[12] A. Ali, G. Kramer, and G.-h. Zhu, Eur. Phys. J. C **47**, 625 (2006).
[13] C. Bobeth, G. Hiller, and G. Piranishvili, J. High Energy Phys. 07 (2008) 106.
[14] U. Egede, T. Hurth, J. Matias, M. Ramon, and W. Reece, J. High Energy Phys. 11 (2008) 032.
[15] W. Altmannshofer *et al.*, J. High Energy Phys. 01 (2009) 019.
[16] C. W. Chiang, R. H. Li, and C. D. Lu, arXiv:0911.2399.
[17] A. K. Alok, A. Dighe, D. Ghosh, D. London, J. Matias, M. Nagashima, and A. Szynkman, J. High Energy Phys. 02 (2010) 053.
[18] Q. Chang, X. Q. Li, and Y. D. Yang, J. High Energy Phys. 04 (2010) 052.
[19] A. Bharucha and W. Reece, Eur. Phys. J. C **69**, 623 (2010).
[20] A. Khodjamirian, T. Mannel, A. A. Pivovarov, and Y. M. Wang, J. High Energy Phys. 09 (2010) 089.
[21] C. Bobeth, G. Hiller, and D. van Dyk, J. High Energy Phys. 07 (2010) 098.
[22] A. K. Alok, A. Datta, A. Dighe, M. Duraisamy, D. Ghosh, D. London, and S. U. Sankar, arXiv:1008.2367.
[23] S. Rai Choudhury *et al.*, Phys. Rev. D **74**, 054031 (2006).
[24] S. R. Choudhury, A. S. Cornell, and N. Gaur, Phys. Rev. D **81**, 094018 (2010).
[25] H. Hatanaka and K. C. Yang, Phys. Rev. D **79**, 114008 (2009).
[26] H. Hatanaka and K. C. Yang, Eur. Phys. J. C **67**, 149 (2010).
[27] W. Wang, Phys. Rev. D **83**, 014008 (2011).
[28] T. G. Rizzo, Phys. Rev. D **33**, 3329 (1986).
[29] G. C. Branco and L. Lavoura, Nucl. Phys. **B278**, 738 (1986).

[30] P. Langacker and D. London, Phys. Rev. D **38**, 886 (1988).
[31] M. Shin, M. Bander, and D. Silverman, Phys. Lett. B **219**, 381 (1989).
[32] Y. Nir and D. J. Silverman, Phys. Rev. D **42**, 1477 (1990).
[33] G. Barenboim and F. J. Botella, Phys. Lett. B **433**, 385 (1998).
[34] G. Barenboim, F. J. Botella, and O. Vives, Nucl. Phys. **B613**, 285 (2001).
[35] C. H. Chen, C. Q. Geng, and L. Li, Phys. Lett. B **670**, 374 (2009).
[36] R. Mohanta and A. K. Giri, Phys. Rev. D **78**, 116002 (2008).
[37] P. Langacker and M. Plumacher, Phys. Rev. D **62**, 013006 (2000).
[38] V. Barger, C. W. Chiang, P. Langacker, and H. S. Lee, Phys. Lett. B **580**, 186 (2004).
[39] C. W. Chiang, N. G. Deshpande, and J. Jiang, J. High Energy Phys. 08 (2006) 075.
[40] V. Barger, L. Everett, J. Jiang, P. Langacker, T. Liu, and C. Wagner, Phys. Rev. D **80**, 055008 (2009).
[41] V. Barger, L. L. Everett, J. Jiang, P. Langacker, T. Liu, and C. E. M. Wagner, J. High Energy Phys. 12 (2009) 048.
[42] P. Langacker, Rev. Mod. Phys. **81**, 1199 (2009).
[43] K. C. Yang, Phys. Lett. B **695**, 444 (2011).
[44] H. Y. Cheng, Y. Koike, and K. C. Yang, Phys. Rev. D **82**, 054019 (2010).
[45] Y. Y. Keum, H. n. Li, and A. I. Sanda, Phys. Lett. B **504**, 6 (2001); Phys. Rev. D **63**, 054008 (2001); C. D. Lu, K. Ukai, and M. Z. Yang, Phys. Rev. D **63**, 074009 (2001); C. D. Lu and M. Z. Yang, Eur. Phys. J. C **23**, 275 (2002).
[46] Z. G. Wang, arXiv:1011.3200.
[47] C. H. Chen, C. Q. Geng, and W. Wang, J. High Energy Phys. 11 (2010) 089.
[48] E. Barberio *et al.* (Heavy Flavor Averaging Group), arXiv:1010.1589. The updated results can be found at www.slact.stanford.edu/xorg/hfag.
[49] K. Nakamura *et al.* (Particle Data Group), J. Phys. G **37**, 075021 (2010).
[50] G. Buchalla, A. J. Buras, and M. E. Lautenbacher, Rev. Mod. Phys. **68**, 1125 (1996).
[51] V. M. Abazov *et al.* (D0 Collaboration), Phys. Lett. B **693**, 539 (2010).
[52] A. J. Buras and M. Munz, Phys. Rev. D **52**, 186 (1995).
[53] C. S. Lim, T. Morozumi, and A. I. Sanda, Phys. Lett. B **218**, 343 (1989).
[54] A. Ali, T. Mannel, and T. Morozumi, Phys. Lett. B **273**, 505 (1991).
[55] C. D. Lu and D. X. Zhang, Phys. Lett. B **397**, 279 (1997).